

Metabolic and evolutionary engineering of a xylose-fermenting strain of

Saccharomyces cerevisiae

Janet Pecháček

A Thesis

in

The Department

of

Biology

Presented in Partial Fulfillment of the Requirements
for the Degree of Master of Science (Biology) at
Concordia University
Montréal, Québec, Canada

November 2011

© Janet Pecháček, 2011

CONCORDIA UNIVERSITY

School of Graduate Studies

This is to certify that the thesis prepared

By: Janet Pechacek

Entitled: Metabolic and evolutionary engineering of a xylose-fermenting strain of
Saccharomyces cerevisiae

and submitted in partial fulfillment of the requirements for the degree of

Master of Science (Biology)

complies with the regulations of the University and meets the accepted standards with respect to originality and quality.

Signed by the final examining committee:

_____ Chair
Dr. D. Walsh

_____ External Examiner
Dr. J. Powlowski

_____ Examiner
Dr. R. Storms

_____ Examiner
Dr. P. Joyce

_____ Thesis Supervisor
Dr. V. Martin

Approved by: _____
Dr. S. Dayanandan, Graduate Program Director

November 8th, 2011 _____
Dr. B. Lewis, Dean of Faculty of Arts and Science

ABSTRACT

Metabolic and evolutionary engineering of a xylose-fermenting strain of *Saccharomyces cerevisiae*

Janet Pechacek

Lignocellulosic biomass waste is an abundant renewable resource of sugars for fermentation to biofuel. Due to its high fermentation capability and tolerance to ethanol and inhibitors, *Saccharomyces cerevisiae* was chosen to engineer a strain able to ferment xylose to ethanol. Wild-type *S. cerevisiae* is not able to grow on xylose as a sole carbon source. In xylose-fermenting yeasts, xylose reductase reduces the sugar to xylitol, which is then oxidized to xylulose by a xylitol dehydrogenase. These two enzymes require different cofactors, which leads to a cofactor imbalance in wild-type cells attempting to utilize xylose. In order to bypass the two-step oxidoreductive isomerization reaction, the xylose reductase-encoding *GRE3* gene was knocked out and the pathway was replaced with a xylose isomerase (*XYLA*) isolated from *Piromyces* sp. E2, to convert xylose directly to xylulose. To increase the flux of xylulose towards the pentose phosphate pathway, a second copy of the endogenous xylulokinase (*XKS1*) was constitutively expressed. This two-gene construct was chromosomally integrated into the *GRE3* deletion strains and the resulting strain was able to grow aerobically on xylose as its sole carbon source. Anaerobic glucose-xylose co-fermentation experiments yielded increased growth as compared to glucose only cultures, but ethanol production did not increase. In micro-aerobic high cell density fermentation the strains successfully produced ethanol from xylose as its sole carbon source and from a mixture of glucose and xylose. Evolutionary engineering further improved the growth rate, ethanol yield and specific ethanol productivity of these strains.

Acknowledgements

First and foremost, I have to thank my supervisor Dr. Vincent Martin for his guidance and support, as well as for the collaborative research environment he has created. Thank you also, to our research and administrative assistant Ada Sijercic for making our lives so much easier.

I would also like to thank Dr. Reginald Storms and Dr. Paul Joyce for sitting on my committee.

Thank you to all the lab members past and present for their support and for being such a great group of friends with such diverse personalities. Special thanks to Nicholas Gold for constructing the *GRE3* deletion strains, to Dr. Caroline Wilde for sharing her knowledge, her guidance and friendship and her delta4swal sequence and to Dominic Pinel and Dr. Andy Ekins for their expert advice. Special thanks also goes to Yun (Sugar Mama) and Linda for their sugary treats.

I would also like to thank my Air Canada family for their encouragement and confidence and for their efforts to accommodate my need for time-off work during the past three years. Special gratitude goes to Bill Watt for his interest in my work and his tasty lunches.

Most importantly I would like to acknowledge my family: my mother and sister for their sacrifices, encouragement, emotional support and confidence in me and my late father for teaching me patience. I also have to hold him responsible for my interest in science.

Table of Contents

ABSTRACT	iii
Acknowledgements.....	iv
LIST OF FIGURES	vii
LIST OF TABLES	ix
LIST OF EQUATIONS	ix
LIST OF ABBREVIATIONS.....	x
1. Rationale and objectives	1
2. Introduction	2
2.1. Bioconversion of cellulosic biomass	2
2.2. Xylose-fermenting microorganisms	3
2.3. Engineered and evolved xylose fermentation in <i>Saccharomyces cerevisiae</i>	8
3. Materials and Methods.....	13
3.1. Strains and media	14
3.2. Metabolic engineering	16
3.2.1. <i>GRE3</i> deletion	16
3.2.2. Xylose fermentation pathway construction	17
3.2.3. Chromosomal integration of the xylose pathway	21
3.3. Strain characterization	23
3.3.1. Reverse transcription PCR	23
3.3.2. Analytical methods	24
3.3.3. Determination of physiological parameters.....	26
3.4. Evolutionary engineering.....	28
4. Results	32
4.1. Base strain construction	32
4.1.1. <i>GRE3</i> deletion	32
4.1.2. Construction of the xylose fermentation pathway.....	33
4.1.3. Chromosomal integration of the xylose fermentation pathway.....	35
4.2. Base strain characterization.....	37
4.2.1. Reverse transcription PCR	37
4.2.2. Growth on xylose of the metabolically engineered base strains	39
4.2.3. Oxygen requirement of the metabolically engineered base strains	41
4.3. Mutagenesis.....	42
4.4. Characterization of the mutant strains.....	44

4.4.1. Adaptation to oxygen-limited conditions.....	44
4.4.2. Glucose-xylose co-fermentation.....	47
4.4.3. High cell density sugar fermentations.....	48
5. Discussion.....	59
6. References.....	72
Appendix A.....	82

LIST OF FIGURES

No.	Page no.
1. Schematic model of the bacterial xylose conversion pathway	4
2. Schematic model of the eukaryotic xylose conversion pathway	7
3. Metabolic engineering targets	14
4. <i>GRE3</i> deletion strategy	16
5. Schematic representation of the pGREGXKXI construction strategy by homologous recombination in yeast	18
6. Illustration of the xylose utilization expression vector: pGREGXKXI	19
7. Illustration of the integration vector: pUC19XKXIURA3delta4swal	21
8. HPLC graph of a standard sample	25
9. HPLC standard curves	26
10. <i>GRE3</i> deletion: ethidium bromide stained agarose gel of PCR amplified fragments	33
11. Restriction enzyme digest pattern of the assembled plasmid isolated from three clones of <i>E. coli</i> pGREGXKXI	33
12. PCR products resolved on an agarose gel stained with ethidium bromide using pGREGXKXI isolated from three <i>E.coli</i> clones	34
13. Restriction enzyme digestion pattern of pGREGXKXIdelta4SwaIURA3 and pUC19 digested with <i>EcoRI</i> and <i>PfoI</i> , and of the integration plasmid pUC19XKXIURA3delta4SwaI digested with <i>SwaI</i>	35
14. Schematic representation of the integration of the linearized plasmid pUC19XKXIdelta4SwaIURA3 into a delta4 site of the yeast chromosome	36

15. Agarose gel resolved PCR product using genomic DNA extracted from various clones positive for the chromosomal integration of the <i>XKS1-XYLA-URA3</i> construct.....	36
16. Ethidium bromide stained agarose gels of RNA isolated from 13d pGREGXKXI grown in different media.	37
17. Ethidium bromide stained agarose gel of the reverse transcription PCR results	38
18. Aerobic growth curve of 13d pGREGXKXI on minimal media supplemented with xylose or glucose.	40
19. Aerobic growth of base strains 13dΔGRE3XKXI and 5dΔGRE3XKXI on minimal media supplemented with xylose	40
20. Oxygen dependent growth on xylose of 5dΔGRE3XKXI, 13dΔGRE3XKXI and control strains 5dΔGRE3 and 13dΔGRE3 in media with different oxygen concentrations.....	41
21. Adaptation to decreasing oxygen availability of 5dΔGRE3XKXI, 13dΔGRE3XKXI and mixed mutant populations 5dΔGRE3XKXI and 13dΔGRE3XKXI in minimal media supplemented with xylose.	45
22. Correlation between the final optical density reached and oxygen availability of mixed mutant populations	46
23. Anaerobic fermentations of mixed mutant populations of <i>MATα</i> and <i>MATa</i> and of the <i>MATα</i> base strain in minimal media supplemented with glucose and xylose or glucose alone.	48
24: High cell density fermentation of base strains, mixed mutant populations, and mutant populations enriched for growth on xylose in minimal media supplemented with xylose, glucose, or both xylose and glucose	49

LIST OF TABLES

No.	Page no.
1. Mutagenesis results: number of colonies on plates irradiated with 10000, 7500, or 0 μJ of UV light and incubated either aerobically or anaerobically	43
2. Summary of results of the high cell density fermentation experiment	51
3. Performance of metabolically-engineered and xylose-adapted strains of <i>S. cerevisiae</i> in fermentation experiments.....	70

LIST OF EQUATIONS

No.	Page no.
1. Estimation of the ethanol yield attributable to xylose fermentation in the mixed sugar cultures	27
2. Specific ethanol productivity.....	27
3. Specific xylose uptake rate	28

LIST OF ABBREVIATIONS

ADH	Alcohol dehydrogenase
CYC1	Cytochrome C1
DCW	Dry cell weight
<i>frd</i>	Fumarate reductase gene
HPLC	High performance liquid chromatography
KanMX	Kanamycin/G418 resistance cassette
LB	Luria Bertani
LDH	Lactate dehydrogenase
OD ₆₀₀	Optical density at 600 nanometer wavelength
PET	Production of ethanol operon
PDC	Pyruvate decarboxylase
PFL	Pyruvate formate lyase
PGI	Phosphoglucose isomerase
RT-PCR	Reverse transcription polymerase chain reaction
<i>talB</i>	Transaldolase
TEF	Transcriptional elongation factor
<i>tktA</i>	Transketolase
TPI	Triose phosphate isomerase
URA3	Uracil auxotrophic marker
UV	Ultraviolet
XDH	Xylitol dehydrogenase
XI	Xylose isomerase
XKS	Xylulokinase
XR	Xylulose reductase
<i>xylA</i>	Xylose isomerase gene
<i>xylB</i>	<i>E. coli</i> xylulokinase gene
YNB	Yeast nitrogen base
YPD	Yeast extract peptone dextrose
5-FOA	5-fluoroorotic acid

1. Rationale and objectives

The aim of this project was to engineer *Saccharomyces cerevisiae* for ethanolic fermentation of the pentose sugar xylose using a combination of rational design and evolutionary engineering approaches. In the metabolic engineering part of this work, a functional xylose utilization pathway was engineered through the chromosomal integration of an exogenous xylose isomerase gene in conjunction with the over-expression of the endogenous xylulokinase to increase the flux of xylose to the pentose phosphate pathway. The xylose reductase gene was deleted to limit the generation of the by-product xylitol. Next, this strain was subjected to evolutionary engineering to improve its xylose utilization and ethanol production. Due to the limited knowledge available on gene targets that may affect this novel metabolic pathway in *S. cerevisiae*, random mutagenesis was employed to generate a genetically variable library of mutants with potentially improved xylose utilization and fermentation performance. The effect on the desired phenotype of prolonged incubation periods in xylose-containing medium was also investigated, as this may result in further improvements through natural adaptation or spontaneous mutations arising in these populations, possibly allowing for the enrichment of individual improved strains in these cultures.

2. Introduction

2.1. Bioconversion of cellulosic biomass

Since human consumption of fossil fuels has exceeded the rate at which new reserves are discovered, the need for developing a cost effective way to produce energy from renewable resources has acquired an unprecedented sense of urgency. First generation biofuels have been heavily criticized for their use of food crops as feedstock for fuel production [1, 2]. Increasing the area of farm land being dedicated to growing fuel-crops resulted in increasing water, fertilizer and pesticide use, negating the claim that biofuel was an environmentally friendly alternative to fossil fuels [3, 4, 5]. Lignocellulosic biomass is a cheap and abundant resource that can be obtained from agricultural and industrial waste materials, thus greatly reducing the economic and environmental effects of food crop use. One hurdle in the bioconversion of these materials to fuel is the recalcitrance of this biomass. Therefore, extensive efforts are underway to develop cost-effective technology [6]. Lignocellulosic biomass is mostly composed of cellulose, hemicelluloses and lignin. Cellulose is a homopolymer of glucose residues, while hemicellulose is a heteropolymer composed of various hexoses (glucose, galactose, mannose, rhamnose, and fructose) and pentoses (xylose and arabinose). Individually, these monomeric sugars can be fermented by various microorganisms, but first need to be released through pre-treatment, followed by chemical or enzymatic hydrolysis to become available to fermenting organisms. This step generates many inhibitory compounds, such as lignin residues, acids and aldehydes [7]. Due to the

diverse sugar content and inhibitory compounds, the ideal bioconversion organism should possess several qualities: it would need to have a wide substrate range (preferably with simultaneous co-utilization of all sugars) with high ethanol yield and productivity on all of these sugars, be tolerant to high inhibitor and ethanol concentrations, require no or minimal nutrient supplementation, be tolerant of low pH and high temperatures. Unfortunately, such an organism has not yet been isolated. In addition, sugar fermentation under anaerobic conditions is necessary, since the accurate dosage of oxygen in hydrolysate fermentation in an industrial setting would increase the cost and be difficult to achieve with these viscous feedstocks [8].

2.2. Xylose-fermenting microorganisms

Bacterial xylose fermentation

Some anaerobic bacteria have the advantage of a wide substrate range and have been found to possess the ability to ferment many of the sugars derived from lignocellulosic feedstocks [9]. They are, however, easily inhibited by high sugar concentrations [10] as well as moderate ethanol concentrations and their low tolerance to inhibitors [11] present in biomass hydrolysates requires a costly hydrolysate detoxification step [12]. In fermentation they produce mixed acid products and ethanol is only a minor product, but some thermophilic anaerobic bacteria are capable of efficient xylose fermentation to near the theoretical maximum ethanol yield.

Thermoanaerobacter ethanolicus for example produces 0.42 g ethanol g xylose⁻¹ at substrate concentrations below 10 g l⁻¹, but ethanol yield decreases to 0.29 g g⁻¹ at a substrate concentration above 20 g l⁻¹ [13]. The bacterial xylose pathway proceeds via a xylose isomerase that converts xylose to xylulose. A xylulokinase then phosphorylates the xylulose to generate xylulose 5-phosphate, which through the action of a transketolase and a transaldolase is shunted into the Entner-Doudoroff pathway to generate pyruvate (Figure 1).

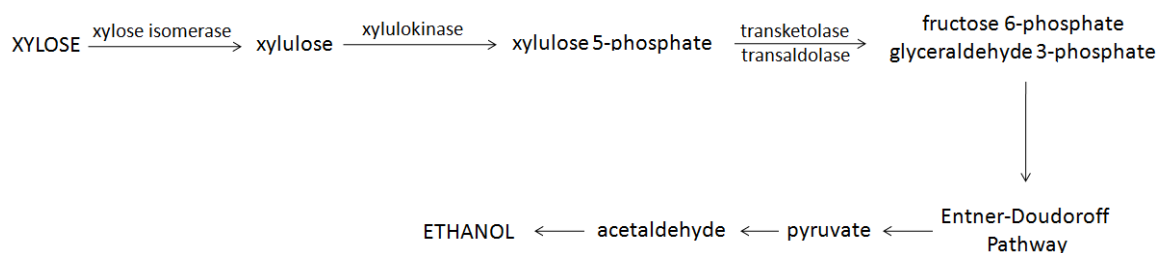


Figure 1. Schematic model of the bacterial xylose conversion pathway, adapted from Dien *et al.* 2003 [14].

While in *Escherichia coli* ethanol is produced from pyruvate using the pyruvate formate lyase (PFL), acetaldehyde dehydrogenase, and alcohol dehydrogenase enzymes, this process requires 2 NADH but only one NADH is produced per pyruvate molecule synthesized. Therefore, in order to maintain NADH balance in the cell large amounts of organic acids are generated. Another disadvantage is the small pH range of 6.0 to 8.0 tolerated by *E. coli* [14]. In 1987, Ingram and his group [15] modified a strain of *E. coli*, such that it produced yeast alcohol dehydrogenase (ADH) and pyruvate decarboxylase (PDC), which requires only one NADH. The resulting *E. coli* strain expressing the PET

(production of ethanol) operon was screened on xylose-containing medium and strain ATC C11303 (pLOI297) was isolated. This strain had increased ethanol tolerance and productivity, but only at a pH above 6.0 [15]. Its narrow tolerable pH range (pH 6.0-8.0) makes its direct application to industrial hydrolysate fermentation questionable [14]. Another attempt to improve the ethanol yield of *E. coli* involved eliminating the endogenous succinate pathway by knocking out the *frd* (fumarate reductase) gene, in order to reduce the amount of co-product formation. The resulting strain KO11 with the PET operon integrated into the *pfl* (pyruvate formate lyase) site produced large amounts of ethanol, but had stability issues in maintaining the integrated operon and required a neutral pH [16]. Stability issues were circumvented by another group who produced a strain carrying mutations in *pfl* and *ldh* (lactate dehydrogenase), rendering it unable to reduce pyruvate to recycle the NADH [17]. This strain was, therefore, not able to grow fermentatively. When the PET plasmid was expressed in this strain, fermentation was restored and plasmid maintenance could easily be ensured by strict anaerobic conditions [17, 18]. One transformant, FBR5, was able to co-ferment glucose, xylose and arabinose with an ethanol yield of 0.46 g g⁻¹ [18].

Contrary to the mixed ethanol and organic acid fermentation of *E. coli*, *Zymomonas mobilis* has a homoethanolic fermentation pathway. In addition to its high ethanol tolerance it also has a high ethanol yield and specific ethanol productivity from glucose [19]. A major drawback to this organism is that it cannot metabolize xylose. When the *E. coli xyIA* (xylose isomerase) and *xyIB* (xylulokinase) genes are expressed in *Z. mobilis* together with *tktA* (transketolase) and *talB* (transaldolase) to convert xylulose

5-phosphate to intermediates of the Entner-Doudoroff pathway a functional xylose fermentation pathway was created and the strain produced ethanol at a titre 86% of the theoretical maximum [20]. Further improvements were made to this strain, but in spite of high ethanol yields xylitol, acetic acid and lactic acid are co-produced. A major obstacle for this organism is its low acetic acid tolerance in the presence of ethanol [21, 22, 23]. Complete inhibition of xylose utilization and ethanol production in the engineered xylose utilizing strain ZM4(pZB5) was found to occur at acetic acid concentrations of 8.0 g l^{-1} when the pH was below 5.0, which are conditions commonly found in hardwood hydrolysates [24].

Eukaryotic xylose fermentation

Fungi have been considered for industrial pentose fermentation due to two qualities: high tolerance to industrial substrates and natural pentose fermentation ability [25, 26]. Success has been limited by their low ethanol tolerance and high by-product production leading to low ethanol yields. Fungal xylose utilization generally requires the action of three main enzymes. Xylose is first reduced to xylitol by a xylose reductase (XR) followed by xylitol oxidation to xylulose by a xylitol dehydrogenase (XDH). The xylulose is phosphorylated to xylulose 5-phosphate by a xylulokinase and then proceeds to the pentose phosphate pathway (Figure 2) [27].

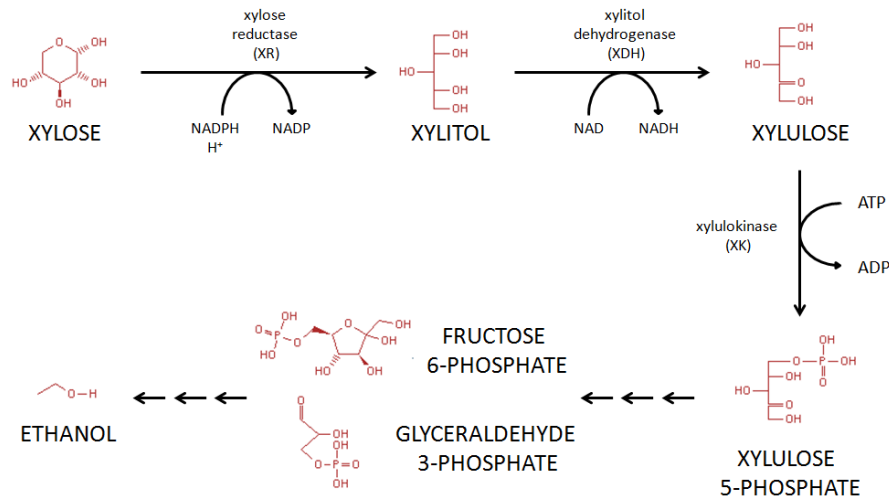


Figure 2. Schematic model of the eukaryotic xylose conversion pathway, adapted from Sonderegger *et al.*, 2004 [54]; Chemical structures reproduced from *Saccharomyces* Genome Database (<http://www.yeastgenome.org>).

One important discovery was that of the anaerobic fungus *Piromyces* sp. E2, the first eukaryote known to date, that has a bacteria-like xylose utilization pathway employing a xylose isomerase for the direct isomerisation of xylose to xylulose [28].

The xylose metabolic pathway in pentose-fermenting yeasts was first described by Gunsalus *et al.* in 1955 [29]. Similar to most fungi, xylose is reduced to xylitol by the action of xylose reductase and subsequently oxidized by xylitol dehydrogenase to xylulose. The xylulokinase then phosphorylates the xylulose to xylulose 5-phosphate which proceeds to the pentose phosphate pathway (Figure 2).

In a 1984 screening study of yeasts isolated from wood sources several organisms were found to ferment xylose to ethanol [30]. The ethanol titres were determined on 20 g l⁻¹ xylose media in 10-day fermentation experiments for *Brettanomyces naardenensis*, *Candida shehatae*, *Candida tenuis*, *Pachysolen tannophilus*, *Pichia segobiensis* and *Pichia*

stipitis. Titres ranged from 1.8 to 6.6 g l⁻¹. The best xylose fermentor in this study was *C. shehatae*, which produced 73% of the theoretical maximum ethanol titre (9 g l⁻¹). Further screening studies for xylose-metabolizing yeasts followed [31, 32, 33, 34, 35] in which *C. shehatae* and *P. stipitis* consistently emerged as the best performers with ethanol yields as high as 0.48 g g⁻¹ or 94% of the theoretical maximum yield for *P. stipitis* in micro-aerobic fermentations [34], and 0.39 g g⁻¹ [36] to 0.45 g g⁻¹ [37] for *C. shehatae* (76-88% of theoretical maximum).

A major issue with the use of pentose-fermenting yeasts for ethanol production from biomass hydrolysates is that they generally require oxygen for efficient xylose utilization [38, 39]. Hydrolysates are viscous, highly concentrated liquids to which the addition of oxygen is not only cost-prohibitive, but also technically challenging. For yeasts to become effective hydrolysate fermenters the engineering of a strain capable of complete anaerobic fermentation is imperative. Another obstacle to the use of xylose-fermenting yeasts for biofuel ethanol production from lignocellulosic hydrolysates is their low ethanol and inhibitor tolerance [40, 41, 42].

2.3. Engineered and evolved xylose fermentation in *Saccharomyces cerevisiae*

Several favourable qualities make *S. cerevisiae* an attractive candidate for the ethanolic fermentation of lignocellulosic substrates. It is a GRAS (Generally Regarded As Safe) organism that has a higher ethanol and inhibitor tolerance than bacteria [43]. It also is capable of efficient glucose fermentation with ethanol yields near the theoretical

maximum. While at least some *S. cerevisiae* strains are able to ferment xylulose, an isomer of xylose, they cannot utilize xylose [39, 44, 45]. Many efforts have been made to engineer a xylose-utilization pathway into this yeast. Shortcomings of these efforts have been attributed to low xylose uptake rates [46], a redox imbalance in the first two steps of xylose metabolism [47], insufficient xylulokinase activity and insufficient activity of the pentose phosphate pathway enzymes [48].

In 1993, Nancy Ho genetically engineered the first strain of *Saccharomyces* sp. able to ferment xylose to ethanol by expressing the *Pichia stipitis* xylose conversion pathway (xylose reductase and xylitol dehydrogenase) together with the endogenous xylulokinase on a plasmid under the control of glycolytic promoters [49]. Her strain was able to produce up to 6 g of ethanol in 60 hrs of fermentation from 4.5 g of xylose and 8.5 g of glucose (0.46 g g⁻¹ of total sugar or 90% of theoretical maximum). Since this first breakthrough, many research groups have attempted to engineer a xylose-fermenting *S. cerevisiae* strain through the expression of the exogenous *P. stipitis* pathway [50, 51, 52, 53, 54, 55]. Some of these efforts are outlined below.

Another group expressed the same pathway in conjunction with the up-regulation of the endogenous xylulokinase in a CEN.PK strain [50]. The resulting strain was named TMB 3001 and had the construct chromosomally integrated. It was, however, only capable of growth on xylose in aerobic conditions. Ethanol yields in anaerobic co-fermentation reached 0.35-0.38 g g⁻¹ (69-75% of theoretical maximum) and a specific ethanol productivity of 0.24-0.30 g g⁻¹ h⁻¹ with different ratios of xylose and glucose in minimal media supplemented with Tween80 and vitamins. The chromosomal

integration of the same genes produced strain TMB 3399, and chemical mutagenesis was performed on this strain [51]. Following enrichment in xylose media, mutants with improved growth rate were obtained. Improvements were observed in ethanol yield and ethanol productivity in both oxygen-limited and anoxic conditions. The best mutant, named TMB 3400, produced 0.25 grams of ethanol per gram of xylose consumed in oxygen limited fermentation and 0.18 grams in completely anoxic conditions, corresponding to 1.2- and 3.6-fold improvements, respectively. Even greater improvements were observed in specific ethanol productivity, which reached $0.10 \text{ g g}^{-1} \text{ h}^{-1}$ in oxygen limited and $0.024 \text{ g g}^{-1} \text{ h}^{-1}$ in anoxic fermentations. This represents a 100-fold and 40-fold improvement over TMB 3399, respectively. When another group of researchers expressed the *P. stipitis* pathway on a plasmid, their strain produced 0.27-0.35 g g^{-1} of ethanol from xylose fermentation and 0.40-0.42 g g^{-1} from xylose-glucose co-fermentation [52]. Evolutionary engineering of TMB 3001, another *S. cerevisiae* strain expressing the *P. stipitis* xylose pathway, yielded TMB 3001 C1, a strain able to co-ferment xylose and glucose to $0.29 \text{ g g}^{-1} \text{ h}^{-1}$. When grown on xylose alone this strain yielded 0.024 g g^{-1} of biomass and 0.277 g g^{-1} of ethanol [53, 54]. The same three genes have also been integrated into a polyploid industrial strain [55]. In anaerobic co-fermentation this strain grew at a faster rate and produced more ethanol compared to TMB 3001 under the same fermentation conditions, reaching 0.27 g g^{-1} (TMB 3001 achieved 0.23 g g^{-1} ethanol yield in this experiment) after 191 hrs.

In 2008 Petschacher and Nidetzky [56] tried a different approach, expressing a xylose reductase from *Candida tenuis* and a xylitol dehydrogenase from *Galactocandida*

mastotermitis in *S. cerevisiae* on different plasmids, and achieved a maximum ethanol yield of 0.34 g g⁻¹ in both oxygen-limited and in anaerobic xylose fermentations of minimal media supplemented with ergosterols and Tween 80.

Walfriedsson (1996) was the first to successfully express a bacterial xylose isomerase in *S. cerevisiae*. The strain expressing the *Thermus thermophilus xylA* gene fermented xylose at an ethanol yield of 0.125 g g⁻¹ (24.5% of theoretical maximum) in minimal media and micro-aerobic conditions, but wasn't able to grow on xylose [57].

Following the discovery of the first xylose isomerase expressing fungus *Piromyces* sp. E2 [28] many advances have been made in expressing this enzyme in *S. cerevisiae* to engineer a functional xylose pathway. Strain RWB 202 expressed the fungal *xylA* gene on a plasmid and achieved an ethanol yield of 0.44 g g⁻¹ in anaerobic glucose-xylose co-fermentation (86% of theoretical maximum ethanol yield) [58]. After evolutionary engineering the spontaneous mutant RWB 202-AFX was isolated and found to be capable of anaerobic ethanolic fermentation with xylose as its sole carbon source with an ethanol yield of 0.42 g g⁻¹ and a more than 10-fold increased growth rate [59]. RWB 217 was constructed to overexpress the *Piromyces* xylose isomerase as well as all enzymes (xylulokinase, ribulose 5-phosphate isomerase, ribulose 5-phosphate epimerase, transketolase and transaldolase) required for the conversion of xylulose to glycolytic intermediates. In addition, the *GRE3* gene encoding the aldose reductase responsible for xylitol production was deleted from this strain. The resulting strain produced 0.43 g g⁻¹ ethanol in both xylose fermentation and in glucose-xylose co-fermentation [60]. This strain was also subjected to evolutionary engineering in glucose-

xylose media and the resulting best mutant produced similar ethanol yields, but had a higher growth rate and biomass yield in xylose medium [61].

Due to the different experimental designs employed in the various efforts to engineer an efficient xylose fermenting *S. cerevisiae* strain outlined here, direct comparisons are not possible. While some researchers performed completely anaerobic fermentations, others applied oxygen-limited conditions. Media composition also differed not only in sugar content and in glucose to xylose ratio for co-fermentation experiments, but in addition, while some used rich media others used defined media supplemented with ergosterols and Tween 80. In general, oxygen-limited fermentations produced more ethanol than anaerobic fermentations, regardless of media composition (except for sugar concentration). For both glucose-xylose and xylose fermentations, yields in minimal media were lower than when fermentation was carried out in rich media.

In spite of the considerable advances made in various research laboratories, the ideal strain of *S. cerevisiae* for the fermentation of lignocellulosic hydrolysates has not yet been engineered. The lignocellulosic biofuel industry would benefit from further improvements in inhibitor tolerance, ethanol yields and productivities, and the ability to ferment pentoses in completely anaerobic conditions without media supplementation. In this work, we attempt to engineer a xylose-fermenting strain of *S. cerevisiae* with increased fermentation capabilities using a combination of metabolic and evolutionary engineering.

3. Materials and Methods

The general strategy for constructing *Saccharomyces cerevisiae* strains able to ferment xylose to ethanol involved two main steps: First, a functional xylose utilization pathway was constructed using a metabolic engineering approach; second, evolutionary engineering techniques were employed in order to improve xylose fermentation. For the engineering of a functional xylose metabolism pathway three steps were required. First, the *GRE3* gene encoding a non-specific aldose reductase capable of reducing xylose to xylitol was deleted, since xylitol production reduces the ethanol yield from xylose. Second, an exogenous xylose isomerase gene (*XYLA*) from the fungus *Piromyces* sp. E2 is chromosomally integrated. Third, the endogenous xylulokinase was up-regulated by introducing a second copy of the native *XKS1* gene under the control of the strong constitutive promoter of the *TPI* gene in order to increase the flux of xylulose towards the pentose phosphate pathway (Figure 3).

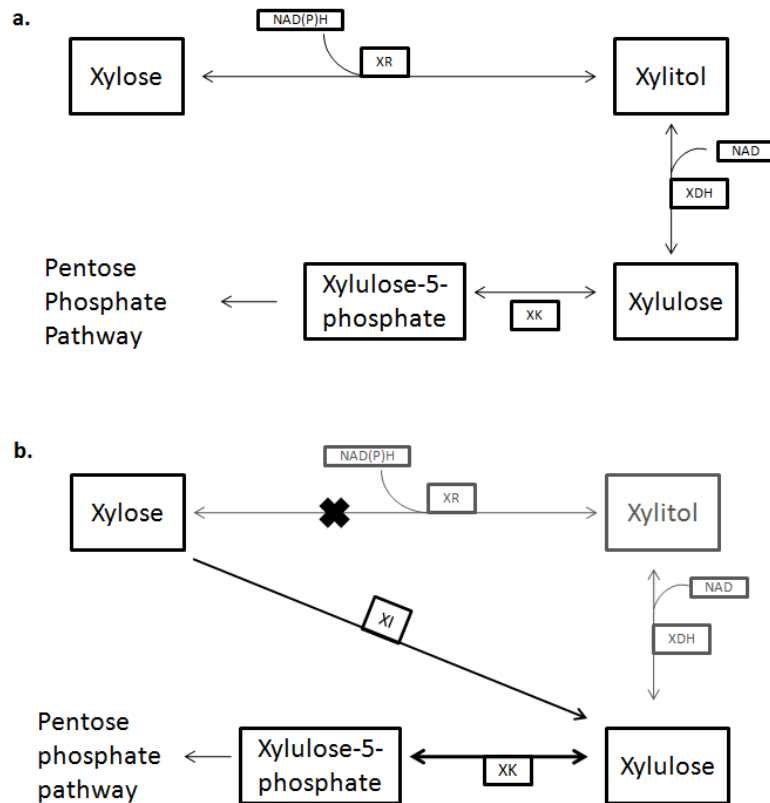


Figure 3. Metabolic engineering targets: a. the native xylose conversion pathway of pentose fermenting yeasts, in which xylose is reduced to xylitol by xylose reductase (XR), followed by the oxidation of xylitol to xylulose by the xylitol dehydrogenase (XDH); b. engineered xylose conversion pathway with the native aldose reductase encoding *GRE3* gene knocked out and xylose is converted directly to xylulose by the exogenous xylose isomerase (XI).

3.1. Strains and media

All genetic changes were introduced into the *Saccharomyces cerevisiae* lab strains CEN.PK113 -5d (*MAT α* , *ura3-52*) and -13d (*MAT α* , *ura3-52*), obtained from Euroscarf (Frankfurt, Germany). These are haploid isogenic strains of opposite mating types that are auxotrophic for uracil. Plasmid propagation was carried out in *Escherichia coli* strain DH5 α . Gene assembly of the *XYLA-XKS1* construct was carried out in *S. cerevisiae* CEN.PK113 -13d using the DNA assembler method [68].

E. coli was grown in Luria Bertani (LB) medium (10 g l⁻¹ tryptone, 5 g l⁻¹ yeast extract, 10 g l⁻¹ sodium chloride). For the selection of cells transformed with plasmids, ampicillin was added to the medium to a final concentration of 50 µg ml⁻¹. *S. cerevisiae* was grown in YPD (10 g l⁻¹ yeast extract, 20 g l⁻¹ peptone, 20 g l⁻¹ dextrose) or in Yeast Nitrogen Base (YNB) supplemented with 50 g l⁻¹ of ammonium sulphate and 20 g l⁻¹ or 40 g l⁻¹ glucose when employing the *URA3* marker for selection and with 20 g l⁻¹ or 40 g l⁻¹ xylose when selecting for a functional xylose utilization pathway. To select against uracil prototrophy YNB was supplemented with 20 g l⁻¹ glucose, 20 mg l⁻¹ uracil and 1 g l⁻¹ 5-fluoroorotic acid (5-FOA). For the induction of *Cre* recombinase YNB was supplemented with 20 g l⁻¹ galactose. Solid media were prepared as above with the addition of agar at a final concentration of 1.5% (w/v). Stocks for strain maintenance were prepared from overnight cultures in LB or YPD for *E. coli* and *S. cerevisiae* respectively, with glycerol added to a final concentration of 15% and frozen at -80°C.

For the reverse transcription PCR experiment, cells were grown in YNB supplemented with 40 g l⁻¹ glucose, 20 g l⁻¹ glucose and 16.6 g l⁻¹ xylose, or 33.3 g l⁻¹ xylose. The xylose concentration was chosen so that all media contained equal amounts of carbon.

3.2. Metabolic engineering

3.2.1. *GRE3* deletion

The Cre-lox system [62] was employed to delete the *GRE3* gene in CEN. PK 113-5d and -13d. To generate a linear deletion construct from pUG72 [63] loxP-*URA3*-loxP was amplified by polymerase chain reaction using primer set FGRE3pUG72 and RGRE3pUG72 (Appendix A), which adds 40 bp of *GRE3* sequence homology immediately upstream and downstream to the PCR product. This construct was transformed into CEN. PK 113-13d and -5d using the lithium acetate method [64]. Selection for uracil prototrophy of transformants was carried out on solid YNB 2% glucose media. Following genomic DNA extraction from several positive clones using the Glass beads method [65], polymerase chain reaction with primers FGRE3OUTpUG6 and RGRE3OUTpUG6 (Appendix A) was performed to confirm correct integration of the deletion construct into the *GRE3* locus.

Next the plasmid pSH47 [62] was transformed into positive Δ *GRE3* *URA*⁺ clones. This plasmid carries both a

URA3 marker and the *Cre* recombinase gene under the inducible *GAL1* promoter. Following a two hour growth period in liquid YPD the cells were transferred into liquid YNB supplemented with 20 g l⁻¹

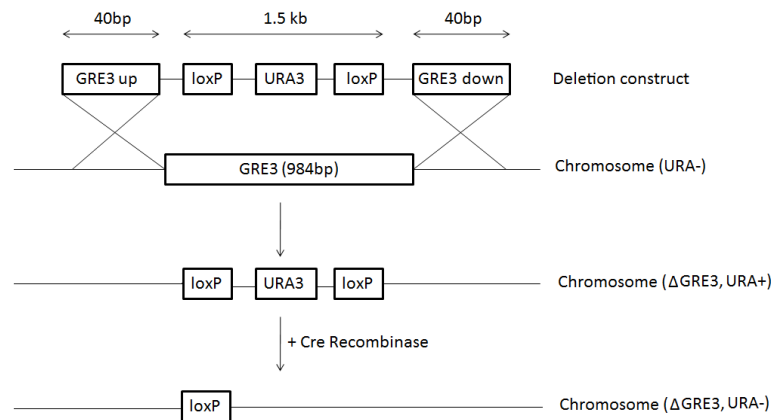


Figure 4. *GRE3* deletion strategy: *GRE3* is knocked out by the loxP-*URA3*-loxP construct by homologous recombination between regions flanking the construct and the *GRE3* open reading frame. The chromosome is cured by the expression of Cre recombinase, which catalyzes the recombination between the two loxP sites, leaving one loxP scar.

galactose and incubated at 30°C with shaking (200 rpm) for two hours in order to induce *Cre* recombinase expression. To select for regeneration of uracil auxotrophy ($\Delta GRE3$ *URA*⁻) the culture was spread on YNB plates supplemented with uracil and with 5-fluoroorotic acid (5-FOA). *URA3* encodes orotidine-5'-phosphate decarboxylase, which converts 5-FOA to the toxic fluorodeoxyuridine allowing for simultaneous selection for the loss of pSH47 and the deletion of the *URA3* marker from the chromosome [66]. Plasmids pUG72 [63] and pSH47 [62] were obtained from the Euroscarf culture collection (<http://web.uni-frankfurt.de/fb15/mikro/euroscarf/index.html>).

3.2.2. Xylose fermentation pathway construction

Plasmid construction:

The *E. coli*-yeast shuttle vector pGREG506 (Euroscarf) [67] was chosen for the assembly and expression of the xylose isomerase encoding *XYLA* gene and the endogenous *XKS1*-encoding xylulokinase. pGREG506 is a CEN-based autosomally replicating, single copy plasmid [67]. The plasmid was linearized by double digestion with *Ascl* and *KpnI* restriction enzymes. *XYLA* was amplified from *Piromyces* sp. E2 genomic DNA with primers XYLfwd and XYLrevCYC (Appendix A). The triosphosphate isomerase (*TPI*) and transcriptional elongation factor (*TEF*) promoters, cytochrome C1 (*CYC1*) and phosphoglucose isomerase (*PGI*) terminators and *XKS1* were amplified from *S. cerevisiae* genomic yeast DNA with primer sets TPIfwd and TPIrev, TEFfwdGREG and TEFrevXKS, CYCfwdXYL and CYCrevGREG, PGI fwd and PGI rev, and XKSfwd and XKSrev,

respectively (Appendix A). Polymerase chain reaction was carried out with Phusion DNA polymerase (Finnzymes, Espoo, Finland) at an annealing temperature of 50°C and an extension time of 15 sec for promoters and terminators, and 80 sec for both genes. To both genes the Kozak sequence AAAACA was added immediately upstream of the start codon.

Plasmid assembly was based on the DNA assembler method [68]. At each end of all fragments, 50 bases of sequence homology corresponding to its neighbouring fragment or to the linearized plasmid backbone was added (Figure 5). Following gel electrophoresis of the six PCR products and of the digested plasmid, the correctly sized bands were cut and purified using the Qiagen gel purification kit (Duesseldorf, Germany). All pieces were then

quantified photometrically using the TECAN nanoquant plate (Maennedorf, Switzerland). Between 1000 and 2000 ng of each fragment together with

2500 ng of the linearized

plasmid were applied to a Millipore spin column with a molecular weight cut-off of 5 kDa (Thermo Scientific, Waltham, MA, USA), centrifuged at 12000 x g for 5 minutes and washed 3 times with sterile de-ionized water to desalt and concentrate the DNA. The resulting approximately 20 µl sample containing the linearized plasmid and all six PCR amplified fragments was transformed into CEN.PK113–13d for assembly by homologous

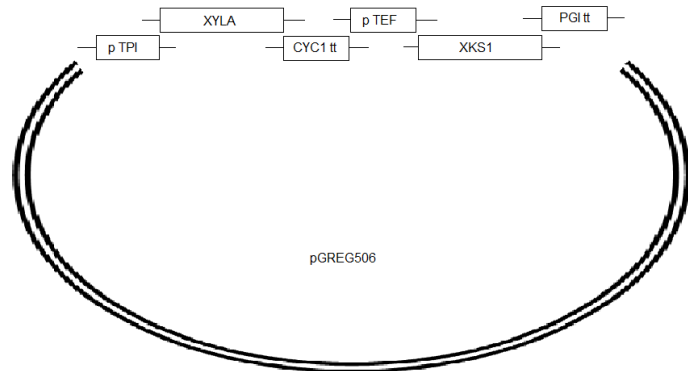


Figure 5. Schematic representation of the pGREGXKXI construction strategy by homologous recombination in yeast

recombination between the regions flanking each fragment using the yeast's recombination machinery. Electrocompetent yeast cells were prepared based on the protocol described by Shao *et al.* [68]. CEN.PK 113-13d was streak purified on YPD plates from -80°C frozen stock. After overnight incubation at 30°C, colonies were used to inoculate 25 ml of YPD medium in a 125 ml Erlenmeyer flask and incubated at 30°C with 200 rpm shaking for 5 hours to an OD₆₀₀ of 1. The cells were then centrifuged at 2000 x g for 5 minutes at room temperature. After washing in 25

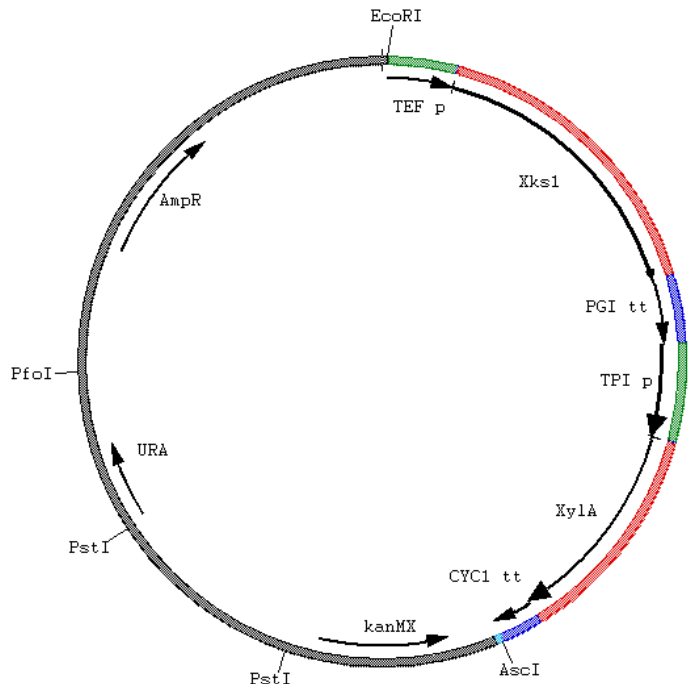


Figure 6. Xylose utilization expression vector: pGREGXKXI

ml cold sterile water, the cells were washed with 1M sorbitol using three cycles of cell suspending and centrifugation at 4000 x g for 1 minute and finally suspended in 250 µL of sorbitol. Fifty µL of cells were used per transformation, carried out in a 2 mm gap electroporation cuvette. After combining the cells and all desalted DNA fragments, the cells were subjected to 1.5 kV, 25 µF, with 200 Ohms electrical resistance using the Bio-Rad GenePulser II (Hercules, MA, USA). One ml of liquid YPD was immediately added and incubated at 30°C for 1 h. The cells were then centrifuged at 2000 x g for 1 min, washed in sorbitol three times as before and plated onto YNB 2% glucose for selection of assembled plasmid bearing cells using the *URA3* marker. Positive clones were

inoculated into 10 ml of YPD and grown at 30°C with 200 rpm shaking for 16 h. The plasmid was isolated using a plasmid miniprep kit from Fermentas (Burlington, Canada) with the following modifications: The pellet obtained from the 16 h culture was suspended in 200 µL of buffer supplied with the kit. Then 100 µL of yeast zymolyase solution and 5 µL of β-mercaptoethanol was added and incubated for 1 h at 37°C and spheroplast formation was confirmed by microscopy. After elution in 30 µL elution buffer supplied with the kit, the plasmid was dialyzed against nanopure water for 20 min on Millipore dialyzing discs with a pore size of 0.025 µm (Thermo Scientific) before electroporation into competent *E. coli* DH5α cells (2.5 kV, 25 µF, 200 Ohms). Plasmid propagation in *E. coli* is necessary to obtain a sufficient concentration for viewing on an ethidium bromide stained agarose gel. Following isolation of the plasmid DNA from *E. coli* clones, correct plasmid assembly was confirmed first by restriction enzyme digestion with *Ascl* and *KpnI* and then by polymerase chain reaction. PCR was performed with Phusion DNA polymerase at an annealing temperature of 50°C and an extension time of 40 sec, using three sets of primers: SQFgreg/CHECKpgiREV, SQF5/SQR8 and SQF8/SQRgreg (Appendix A) to amplify the plasmid from the pGREG backbone to the *PGI* terminator, from *XKS1* to *XYLA* and from the *TPI* promoter to the plasmid backbone. Clones with the correct digestion pattern and PCR bands were sent for sequencing. The correct plasmid was named pGREGXKXI (Figure 6).

PCRs were carried out in the MBS Satellite 0.5G thermocycler (Thermo Scientific). The high fidelity Phusion DNA polymerase (Finnzymes, Espoo, Finland) was used when amplifying DNA for the construction of plasmids and for sequencing; low fidelity Taq

DNA polymerase (Fermentas, Burlington, Canada) was generally used for PCR checks of correct ligations and assemblies. PCR conditions varied with primer sets and with the type of template used, in accordance with the recommendations of the DNA polymerase used.

3.2.3. Chromosomal integration of the xylose pathway

Integration using delta element sequences was chosen for the chromosomal integration of the xylose metabolic pathway. Delta sequences are the integration sites of Ty retrotransposons and are dispersed throughout the genome at more than 400 copies [69]. They tend to be located in gene poor regions and therefore gene disruption is unlikely to occur [69]. This method makes

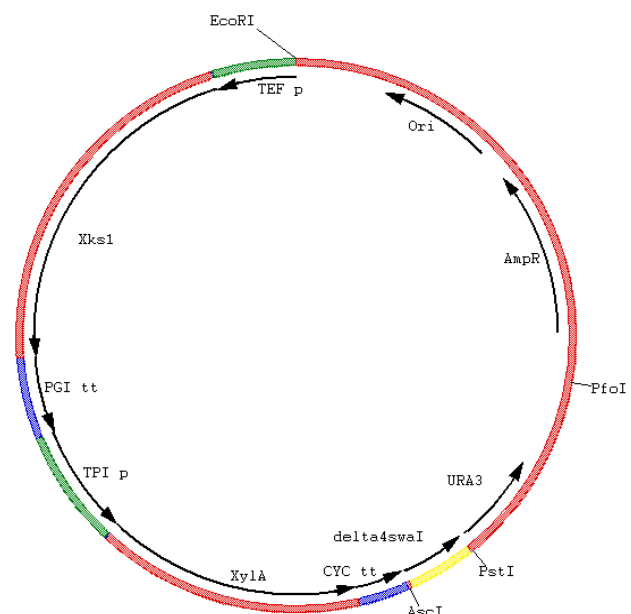


Figure 7. The integration vector: pUC19XKXIURA3delta4swal

for a semi-random integration and also has the advantage of the possibility of multiple integrations, although this is unlikely to occur in our integration due to the large size of our construct, since integration efficiency is reduced with increasing insert size [70].

The delta4 fragment was PCR-amplified from genomic yeast DNA with primers Delta4PfoIFWD2 and Delta4SfoIREV (Appendix A), which added an upstream *PfoI* and a

downstream *SfoI* restriction site and then cloned into pYES2 (Invitrogen, Carlsbad, CA, USA). The fragment was subsequently modified to include a *SwaI* restriction site in its center. This was accomplished by amplifying the two halves of delta4 separately with primers delta4Swalfwd and delta4Swalrev (Appendix A), adding *SwaI* sites downstream of the 5' half and upstream of the 3' half of the delta 4 sequence. Following digestion with *SwaI*, both pieces were ligated together using T4 DNA ligase (Fermentas). The kanamycin resistance (*KanMX*) marker of pGREGXKXI was replaced by the delta4swal sequence by digestion with *AscI* and *PstI*. Since pGREG506 is a single copy plasmid the construct, including the *URA3* marker, was cloned into the *EcoRI* and *PfoI* sites of the high copy-number plasmid pUC19 in order to obtain a large amount of DNA for transformation and integration into the *GRE3* deletion strains. Following linearization of pUC19XKXIURA3delta4swal (Figure 7) by *SwaI* digestion and gel purification using the Qiagen gel purification kit, the construct was dialyzed on Millipore discs for 20 min and electroporated into both *GRE3* deletion strains as described above. Selection for transformants was carried out on YNB 4% glucose plates, employing the *URA3* marker of pUC19XKXIdelta4SwalURA3. Genomic DNA was extracted from several clones of each mating type and chromosomal integration of the construct confirmed by PCR at an annealing temperature of 50°C and 56 sec extension time using Phusion DNA polymerase, with primers SQF8 and SQR11 (Appendix A). All endonucleases used were supplied by New England BioLabs, except for *PfoI*, which was from Fermentas.

3.3. Strain characterization

3.3.1. Reverse transcription PCR

CEN.PK113-13d pGREGXKXI was grown to an OD_{600} of 1 at 30°C with shaking (200 rpm) in 5 ml of 3 different media: 4% glucose, 2% glucose + 1.66% xylose and 3.33% xylose. RNA extraction was performed using the RNeasy Mini Kit from Qiagen and following the provided enzymatic lysis, DNase digestion and RNA clean-up protocols. The resulting RNA was quantified using the TECAN nanoquant plate and normalized across growth conditions for subsequent cDNA synthesis. Superscript reverse transcriptase (Invitrogen) was used in the reaction together with random primers provided in the kit to generate a cDNA library. The library was then used in PCR reactions using three pairs of gene-specific primers (Appendix A): with RTxylApF and RTxylApR amplifying a 150 bp sequence within the *XYLA* gene, RTtpiF and RTtpiR amplifying a 103 bp sequence within the *TPI* gene or promoter, and RTactinF and RTactinR amplifying a 137 bp sequence within the *ACT1* reference gene. Primers were designed using Primer3Plus software (Whitehead Institute for Biomedical Research). Control PCRs were done using genomic DNA isolated from CEN.PK113-13d or RNA that was not reverse transcribed as the template. A control of no nucleic acid added to the reaction mixture was also included.

3.3.2. Analytical methods

Cell growth was monitored by measuring optical density at 600nm (OD_{600}) in a Cary 50 Bio UV visible spectrophotometer (Varian, Santa Clara, California, USA). Glucose, xylose and ethanol concentrations were measured by High Performance Liquid Chromatography (Finnigan Surveyor, Thermo Scientific) with the Aminex HPX-P column (Bio-Rad, Hercules, CA), operated at a flow rate of 0.6 ml min^{-1} , at 85°C with water as the mobile phase. The HPLC was equipped with a refractive index detector (Spectra system RI-150, Thermo Scientific). ChromQuest 5.0 software was used for HPLC data analysis. Standard samples of xylose (2, 1.5, 0.75, 0.6, 0.45, 0.3 and 0.15%), glucose (0.1, 0.08, 0.05, 0.03 and 0.02%), and ethanol (1, 0.5, 0.25, 0.1, 0.05, 0.025 and 0.01%) dissolved in water were loaded on the HPLC to determine their retention times and to determine the lower detection limits of the column and to generate standard curves (Figure 9). A standard sample containing 0.25% xylose and 0.25% glucose and a separate standard sample containing 0.1% ethanol were also loaded to ensure good peak separation of the two sugars (Figure 8). From these results the retention times were determined to be 13.3 min for xylose, 12.2 min for glucose, and 16.6 min for ethanol (Figure 8). The lower detection limits were 0.45% for xylose, 0.01% for glucose, and 0.005% for ethanol, corresponding to the lowest concentration measured for which the concentration vs. peak area still fell within the linear range of the standard curve (Figure 9). Figure 8 also shows the separation between the xylose and glucose peaks.

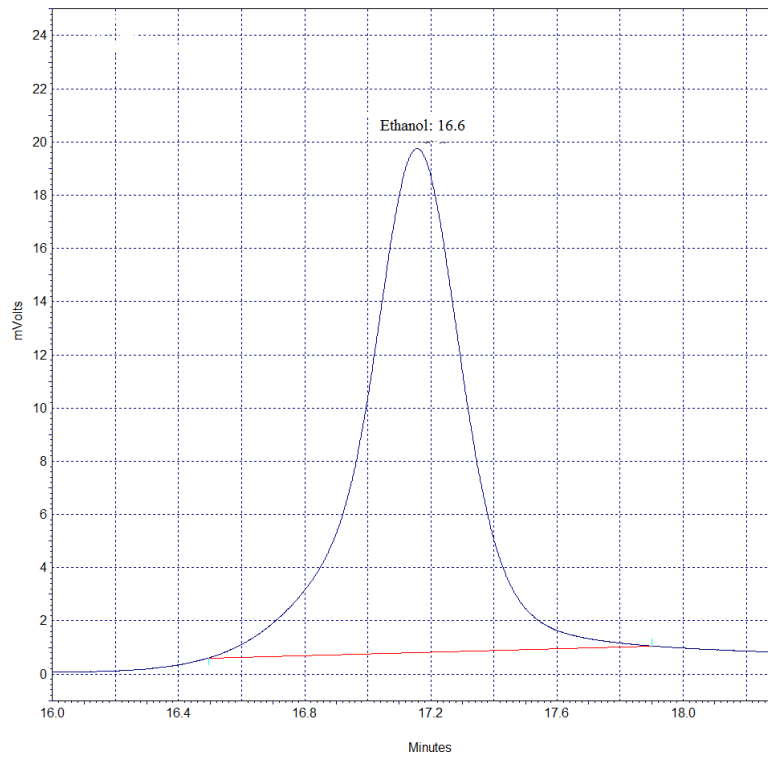
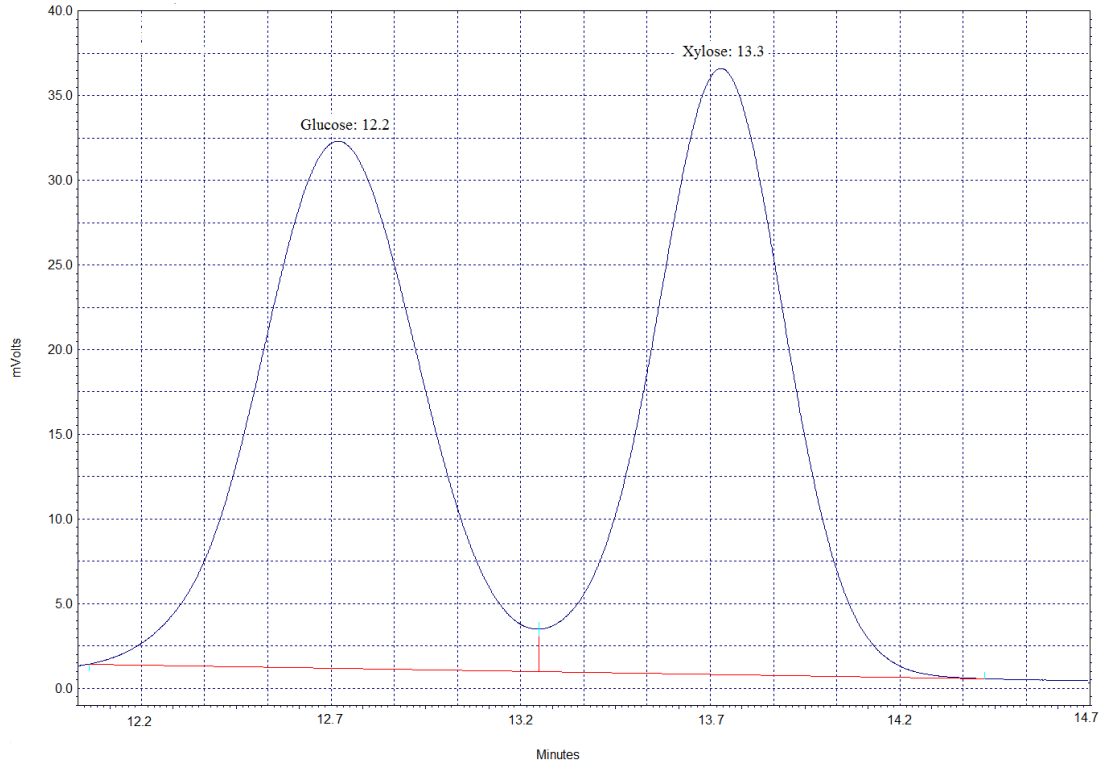


Figure 8. HPLC graph of a standard sample containing 0.25% glucose and 0.25% xylose or 0.1% ethanol resolved on a HPX-P column at 0.6 ml min^{-1} of water.

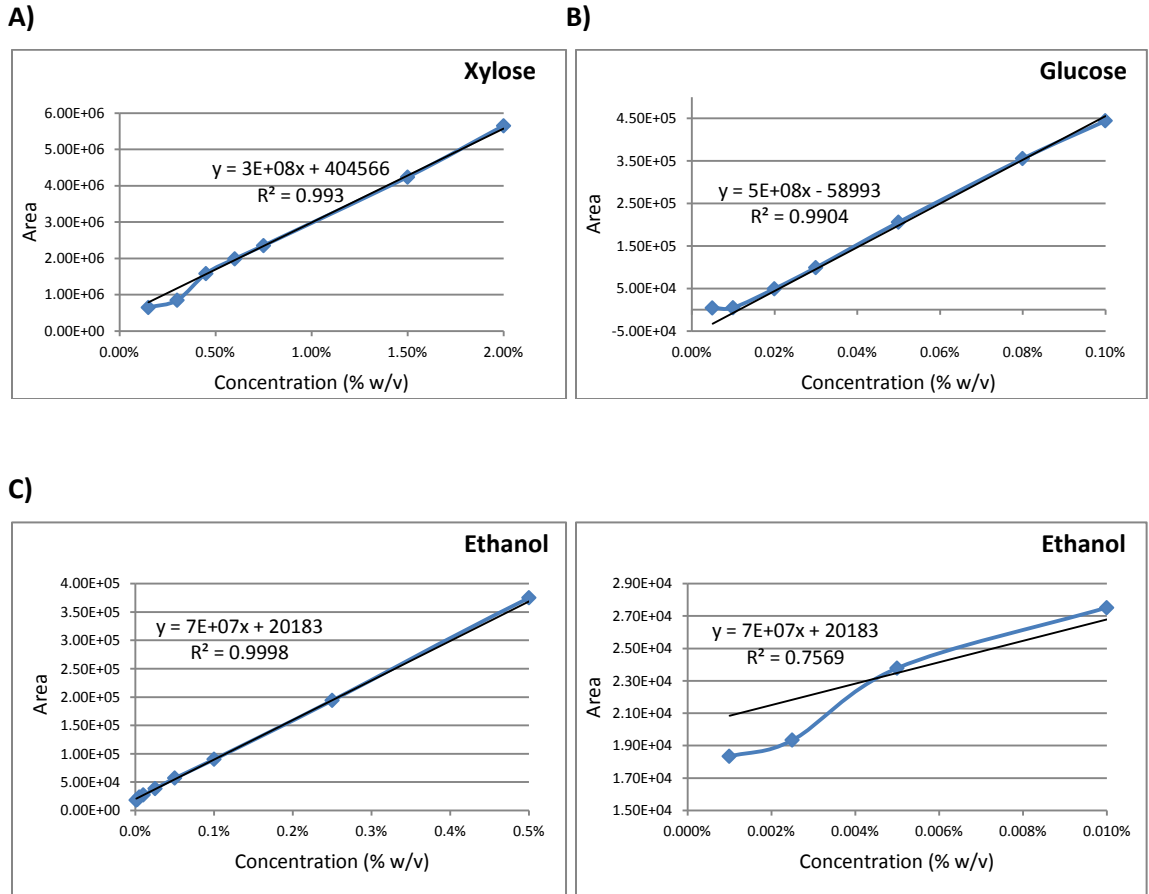


Figure 9. HPLC standard curves of A) xylose, B) glucose, and C) ethanol

Growth rate (μ) was calculated by log-linear regression of the optical density at 600 nm versus time when cells were in exponential growth phase.

Biomass yields (Y_{biomass}) were calculated from the difference between the initial dry cell weight and the dry cell weight at the end of exponential growth, divided by the amount of sugar consumed in the same time period.

Ethanol yields (Y_{ethanol}) were calculated from the difference in ethanol concentration from the time point of initial ethanol detection to the first time point at which the highest ethanol concentration was measured, divided by the total amount of sugar

consumed during the same time period. Assuming that equal amounts of ethanol were produced from the fermentation of glucose in the presence and in the absence of xylose, the ethanol yield from xylose fermentation in the mixed sugar culture ($Y_{x(\text{ethanol})}$) can be estimated. The maximum ethanol concentration measured in the glucose fermentation ($\max C_{\text{ethanol}})_g$ was subtracted from the difference in ethanol concentration from the time point of initial ethanol detection to the time point of highest ethanol concentration in the co-fermentation ($dC_{\text{ethanol}})_{gx}$. This value was then divided by the change in xylose concentration ($dC_{\text{xylose}})_{gx}$ of the co-fermentation culture during the same time period (Equation 1).

$$\text{Eq. 1: } Y_{x(\text{ethanol})} = \frac{(dC_{\text{ethanol}})_{gx} - (\max C_{\text{ethanol}})_g}{(dC_{\text{xylose}})_{gx}}$$

The specific ethanol productivity r_{ethanol} was calculated as the difference in ethanol concentration dC_{ethanol} divided by the time period dt during which this change occurred. This value was divided by the average dry cell weight DCW_{av} for the time points used (Equation 2).

$$\text{Eq. 2: } r_{\text{ethanol}} = \frac{(dC_{\text{ethanol}})}{dt \times DCW_{av}}$$

Similarly, the specific xylose uptake rate was determined by dividing the amount of xylose consumed by the time difference and the average biomass during this time period (Equation 3).

$$\text{Eq. 3: } r_{\text{xylose}} = \frac{(dC_{\text{xylose}})}{dt \times \text{DCW}_{\text{av}}}$$

3.4. Evolutionary engineering

The expression of an exogenous xylose isomerase in *S. cerevisiae* on its own may be sufficient to generate a functional xylose-utilization pathway, but the work of other researchers has demonstrated that more efficient xylose fermentation can be achieved through strain improvement techniques [51, 59, 60]. In this work, strain improvement was attempted by the application of evolutionary engineering techniques. Evolutionary engineering is a strain improvement technique that mimics and attempts to accelerate natural evolutionary processes. In the presence of a strong selection pressure organisms will adapt and/or evolve to increase their fitness in that particular environment. For evolution to take place, the genetic potential for a particular phenotype needs to be present and the novel phenotype must persist and propagate in a population due to increased fitness (i.e. increased survival and/or reproduction rate). Just as natural evolution relies on genetic variability, so does evolutionary engineering. While the existing variability may be sufficient for a population to adapt to a particular

environment, the degree of variability can be increased through the use of mutagens, thus providing the organism with the genetic potential to adapt or evolve more rapidly than natural evolution allows through the occurrence of rare spontaneous mutations.

UV mutagenesis

Following the introduction of a functional xylose-utilization pathway in *S. cerevisiae*, evolutionary engineering was applied to improve the strains' xylose fermentation capability. Ultraviolet irradiation was employed to generate genetic variability (mutations) in the genomes of the two strains with the xylose pathway chromosomally integrated. UV light produces dimers between pyrimidine bases, which interfere with normal base pairing. As a result, the DNA strands cannot be replicated properly and various types of DNA damage can result, including point mutations and deletions [71].

CEN.PK113ΔGRE3 XKXI -5d and -13d were purified from -80°C by streaking onto YPD-agar. Overnight colonies were used to inoculate 5 ml YNB 2% xylose. After normalizing the amount of cells to an OD₆₀₀ of 2 for both cultures, 100 µL were plated on YNB 2% xylose in triplicate and irradiated with 0, 7 500 and 10 000 µJ of UV light using a UV-Stratalinker 1800 (Stratagene, La Jolla, CA, USA). Plates were immediately wrapped in aluminum foil to prevent light-dependent DNA damage repair (photoreactivation) and incubated at 30°C in an anaerobic chamber equipped with a gas analyzer (COY Laboratory products Inc., Grass Lake, MI, USA) until colonies appeared. Control plates irradiated with 10 000 µJ or plates that were not irradiated were incubated aerobically as well.

Growth selection and adaptation

Since neither of the base strains 5dΔGRE3 XKXI and 13dΔGRE3 XKXI were capable of anaerobic growth on xylose as the sole carbon source, I attempted to determine the minimal oxygen requirement of these strains. Air was removed from 90 ml of minimal media in Bellco anaerobic culture bottles (Vineland, NJ, USA) by sparging with nitrogen for ten minutes. After the bottles were capped and sterilized by autoclaving, the media were supplemented with 10 ml of 20% xylose (w/v) solution to a final concentration of 20 g l⁻¹. Using a needle and syringe to pierce through the rubber stopper, 100, 75, 50, or 25 ml of the gas in the bottles was removed and the same volumes of filtered air were reintroduced, resulting in approximately 13.1, 9.9, 6.6, or 3.3% oxygen in the medium (calculated based on an approximate oxygen content of 21% in the atmosphere and assuming 1 atm). One bottle of each oxygen content was inoculated with 5dΔGRE3XKXI, and the other with 13dΔGRE3XKXI. Two extra bottles with 100 ml (13.1% oxygen content) of reintroduced air were prepared and inoculated with 5dΔGRE3 and 13dΔGRE3 control strains. One ml of culture was removed at the beginning of the experiment and at subsequent time points for culture growth measurement by optical density.

In an attempt to adapt the base strains and the UV-generated mixed mutant populations to decreasing oxygen levels, the strains were inoculated into serial cultures of decreasing oxygen concentration. Bellco bottles were prepared as above with 75, 50, 25, 10, 5, and 0 ml of air injected, resulting in media with approximately 9.9, 6.6, 3.3, 1.3, 0.7 and 0% oxygen, respectively. First, the strains were grown aerobically in YNB 2%

xylose for 24 hrs. These pre-cultures were then used to inoculate bottles with 9.9% oxygen to an OD_{600} of 0.05. During logarithmic growth phase of each culture, appropriate volumes were removed in order to inoculate the bottles with the next lowest oxygen content to an OD_{600} of 0.05. One ml of culture was removed for optical density measurement at various time points for all cultures.

Fermentation at high cell densities

In the high cell density fermentation experiments, strains were first grown in 5 ml of YPD medium in test tubes and incubated at 30°C with shaking (200 rpm) for 10 hrs, then transferred into 100 ml YPD in 250 ml Erlenmeyer flasks and incubated for another 12 hrs (30°C, 200 rpm). Cells from the entire culture were washed three times with sterile nanopure water and finally suspended in 5 ml of water. Cell densities were measured by optical density at 600 nm and appropriate volumes were used to inoculate the experimental cultures with 10^9 cells ml^{-1} . These were inoculated into 250 ml Erlenmeyer flasks containing 100 ml of one of three types of media: YNB supplemented with 15 g l^{-1} xylose, 1 g l^{-1} glucose, or both 15 g l^{-1} xylose and 1 g l^{-1} glucose. From these cultures samples were taken at various time points for measurement of optical density, dry cell weight, and for HPLC analysis.

4. Results

4.1. Base strain construction

4.1.1. *GRE3* deletion

In order to increase the efficiency of the xylose fermentation pathway that was introduced into *S. cerevisiae* strains CEN. PK 113 -5d and 13d, we deleted the native *GRE3* gene. Following transformation with the *GRE3* deletion construct (loxP-*URA3*-loxP) amplified from pUG72, transformants were able to grow on minimal media (YNB) supplemented with glucose in the absence of uracil, suggesting that the *URA3* marker was correctly integrated into the *GRE3* locus. PCR of genomic DNA isolated from several transformants of each mating type confirmed correct integration of the construct, resulting in $\Delta GRE3 URA^+$ strains (Figure 10, lanes B and D). When the pSH47 plasmid expressing the *Cre* recombinase was transformed into these strains and *Cre* recombinase expression was induced, transformants positive for the deletion of the *URA3* marker (recombination between the two loxP sites) were able to grow on minimal media supplemented with uracil and 5-FOA, indicating *URA3* deletion from the *GRE3* site of the chromosome ($\Delta GRE3 URA^-$), as well as loss of the *URA3* marker contained in the *Cre* recombinase plasmid (i.e. loss of pSH47). Genomic DNA was extracted from three clones of each mating type to perform PCR and confirm the deletion of *URA3*. Figure 10 shows the PCR products resolved on an agarose gel stained with ethidium bromide. A PCR product of 2040 bp was expected in the wild-type yeast strain (lane A), of 2590 bp if the *GRE3* locus was replaced by loxP-*URA3*-loxP ($\Delta GRE3 URA^+$, lanes B and

D), and finally of 1110 bp if the desired genotype was achieved with *GRE3* deleted and *URA3* removed by the *Cre* recombinase ($\Delta GRE3 URA^-$, lanes C and E).

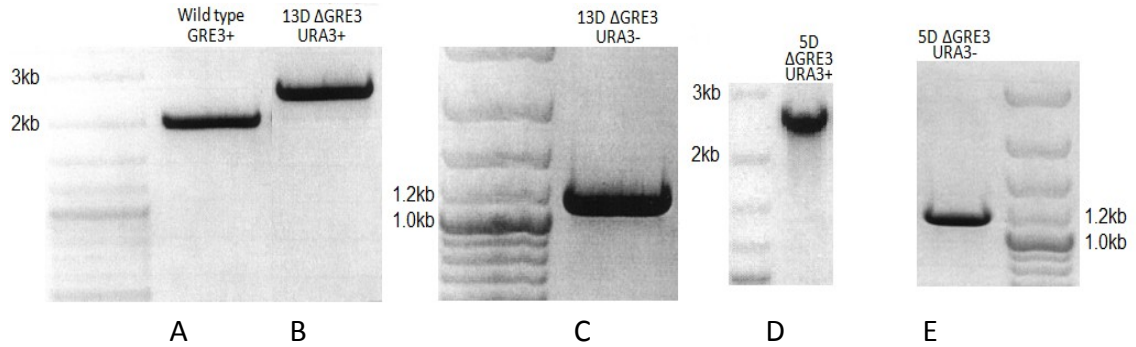


Figure 10. *GRE3* deletion: ethidium bromide stained agarose gels of PCR amplified fragments using primers upstream and downstream of the *GRE3* locus. A) 2040 bp wild-type band; *GRE3* locus replaced by loxPURA3loxP in B) strain 13d and D) strain 5d; *URA3* marker excised by recombination between the two loxP sites in C) strain 5d and E) strain 13d

4.1.2. Construction of the xylose fermentation pathway

To engineer a functional xylose fermentation pathway in *S. cerevisiae*, the endogenous xylulokinase was up-regulated by introducing a second copy of *XKS1* and the exogenous xylose isomerase was introduced by expressing *XYLA*, both under constitutive promoters from a plasmid (Figure 6). Figure 11 shows the restriction enzyme digestion products of three pGREGXKXI clones, confirming correct assembly of the DNA fragments by homologous recombination in

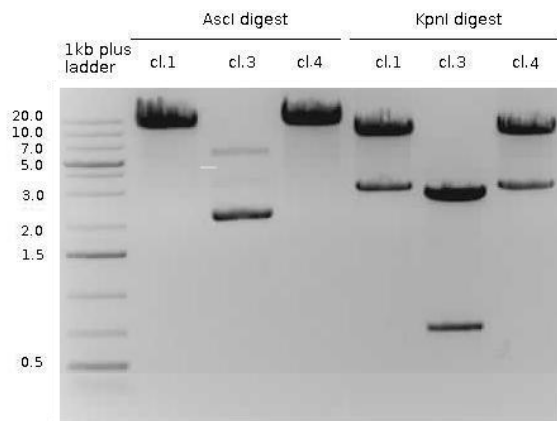


Figure 11. Restriction enzyme digest pattern of the assembled plasmid isolated from three clones of *E. coli* pGREGXKXI

confirming correct assembly of the DNA fragments by homologous recombination in

two of the three clones shown: clones 1 and 4. PCR results conducted on the isolated plasmids with three different sets of primers (Appendix A) targeting three regions of the plasmid concur with the restriction enzyme digest results (Figure 12). Primer set A amplifies a 2.4 kbp region from the pGREG plasmid backbone to the *PGI* terminator, primer set B amplifies a 1.6 kbp region from *XKS1* to *XYLA*, and primer set C amplifies a 1.8 kbp region from the *TPI* promoter to the plasmid backbone. Clones 1 and 4 were sent for sequencing and the resulting sequence for clone 4 proved to be correct, while that of clone 1 contained point mutations, possibly generated during PCR DNA amplification or during plasmid assembly by homologous recombination in yeast.

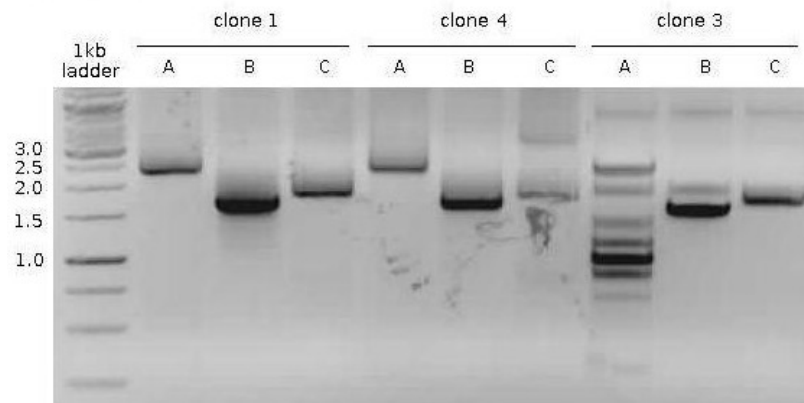


Figure 12. PCR products resolved on an agarose gel stained with ethidium bromide using pGREGXXI isolated from three *E. coli* clones with three different sets of primers: A) amplifies a 2.4 kbp fragment from the pGREG plasmid backbone to the *PGI* terminator, B) amplifies a 1.6 kbp fragment from *XKS1* to *XYLA* and C) amplifies a 1.8 kbp fragment from the *TPI* promoter to the pGREG plasmid backbone.

4.1.3. Chromosomal integration of the xylose fermentation pathway

To ensure that the engineered xylose fermentation pathway is genetically stable and not lost during cell divisions, the pathway was integrated into the genomes of *S. cerevisiae* strains of both mating types.

Following replacement of the KanMX DNA fragment of pGREGXKXI with the delta4 sequence modified to contain a *SwaI* restriction site, the 6.1 kbp *XKS1*-*XYLA*-delta4-*URA3* fragment of pGREGXKXIdelta4*SwaI*URA3 was directionally cloned into *EcoRI* and *PfoI* sites of pUC19. The digestion pattern of both plasmids is shown in Figure 13.

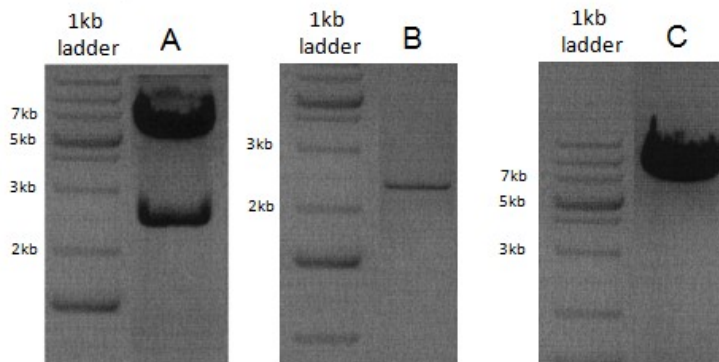


Figure 13. Restriction enzyme digestion pattern of A) pGREGXKXIdelta4*SwaI*URA3 and B) pUC19 digested with *EcoRI* and *PfoI*, and C) *SwaI* digest of the integration plasmid pUC19XKXIURA3delta4*SwaI*

In panel A both the 6.1 kbp XKXIdelta4*SwaI*URA3 fragment and the remaining 2.8 kbp of the pGREG plasmid backbone bands are visible. Panel B shows the 2.3 kbp fragment of the *EcoRI*/*PfoI* double digest of pUC19, the remaining 350 bp band was very

faint. The plasmid resulting from the ligation of the 6.1 kbp pGREGXKXIdelta4SwaIURA3 fragment with the 2.3 kbp pUC19 fragment was linearized by *SwaI* digestion (panel C), which opens it in the middle of the delta4 sequence, thus resulting in the three-gene construct flanked on both end by 150 bp of delta4 sequence for integration into any of the multiple delta4 sites of the chromosomes of both *GRE3* deletion strains (Figure 14).

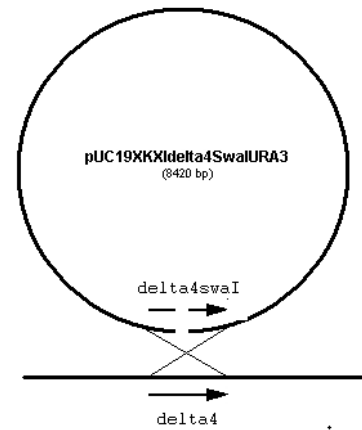


Figure 14: Schematic representation of the integration of the linearized plasmid pUC19XKXIdelta4SwaIURA3 into a delta4 site of the yeast chromosome

Upon transformation with 100 ng of the linearized integration cassette, nine clones of *MAT α* and three of *MAT a* were obtained. PCRs on genomic DNA isolated from these clones using primers SQF8 and SQR11 (Appendix A), which amplify a 1.4 kbp region from the 3' end of the *TPI* promoter to the 3' end of the *XYLA* gene, confirmed chromosomal integration of the cassette (Figure 15). In many clones, multiple PCR products were amplified. For the *MAT α* clone 1 (Cl.1), and for *MAT a* clone 100-2 were chosen and designated as the base strains of this project.

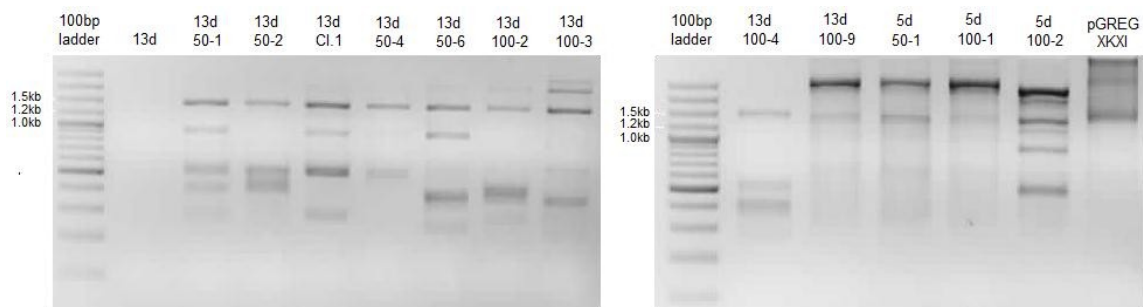


Figure 15. Agarose gel resolved PCR product using genomic DNA extracted from various clones positive for the chromosomal integration of the *XKS1-XYLA-URA3* construct as template.

4.2. Base strain characterization

4.2.1. Reverse transcription PCR

To confirm the constitutive expression of the exogenous xylose isomerase from the expression vector pGREGKXI, reverse transcription PCR was performed. RNA was extracted from cells grown in three different media of equal carbon content: YNB 4% glucose, YNB 2% glucose + 1.66% xylose, and YNB 3.33% xylose. Figure 16-A shows the extraction results with equal volumes (3 μ L) of RNA resolved on an ethidium bromide stained agarose gel. RNA concentrations attained were 436, 596, and 86 $\text{ng } \mu\text{l}^{-1}$ in the extracts from glucose, glucose + xylose, and xylose grown cells, respectively. The RNA concentration was normalized across the different growth conditions (Figure 16-B) for subsequent cDNA synthesis.

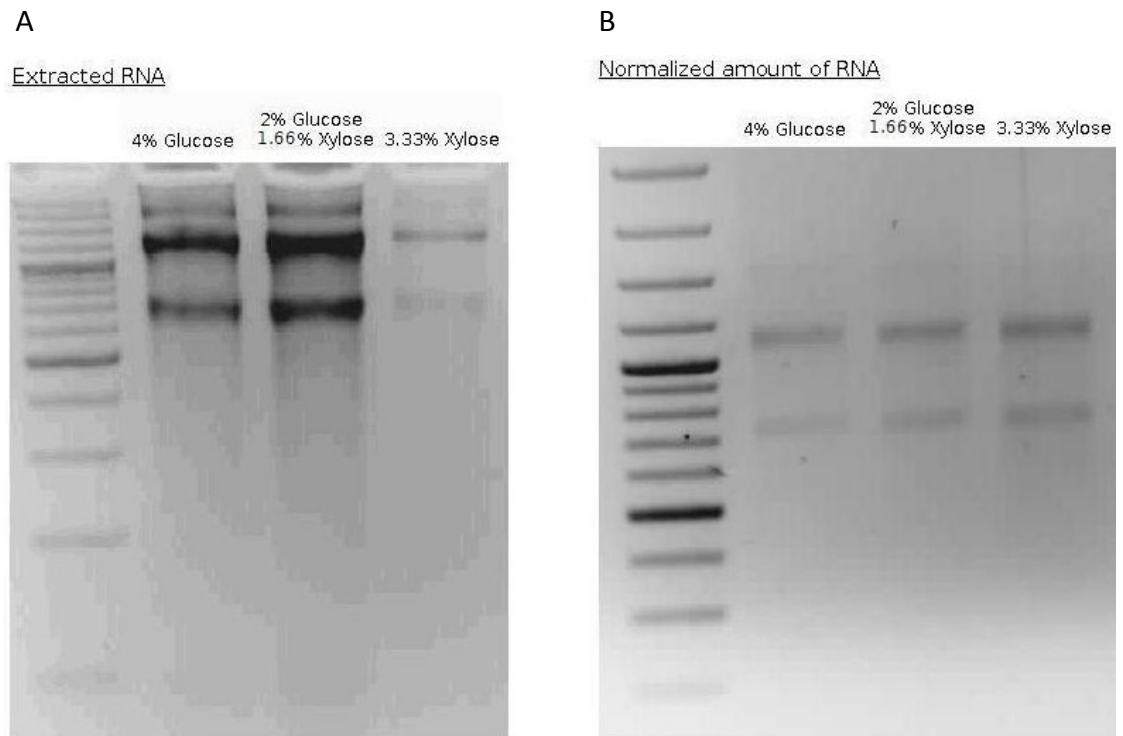


Figure 16. Ethidium bromide stained agarose gel of A) total RNA isolated from 13d pGREGKXI grown in different media and B) normalized amounts of RNA for reverse transcription PCR.

RT-PCR on CEN. PK113 -13d pGREGKXI confirms constitutive *XYLA* transcription even in the absence of xylose, as evidenced by the amplification of the correctly sized DNA fragment from reverse transcribed RNA in all three media (Figure 17A).

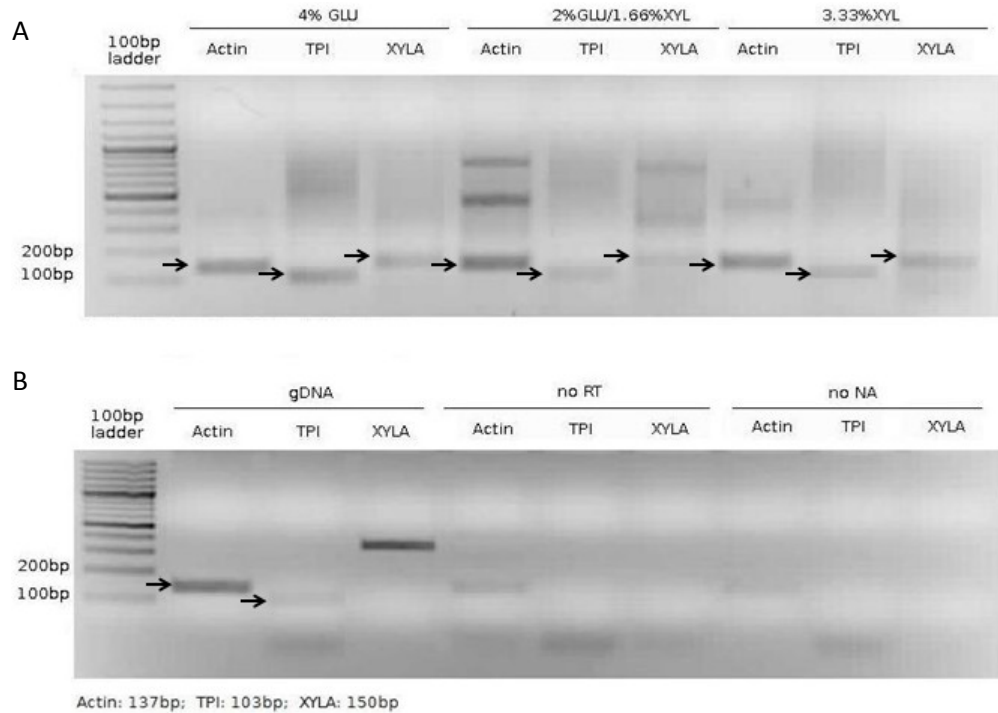


Figure 17. Ethidium bromide stained agarose gel of the reverse transcription PCR results of A) the RNA isolated from cells grown in different media and B) of control PCR reactions with genomic DNA, RNA that was not reverse transcribed and in the absence of any nucleic acid template.

Since the *ACT1* (actin) reference gene expression is not consistent across the different media, these results cannot be used to quantify the abundance of specific RNA in cells grown in media with different sugar compositions. Since both *TPI1* and *XYLA* gene expression is controlled by the same promoter, their expression should

theoretically be comparable, but this is not the case. Regardless of band intensity, these results prove that *XYLA* is constitutively expressed. Control PCRs on genomic DNA show that while the actin primers produce a strong band, the *TPI1* primers appear to not be as efficient. Since the primers for both of these genes could not be designed to span an exon-exon boundary, they are expected to amplify the same-sized fragment of genomic DNA. The *XYLA* primer pair amplifies DNA in the genomic control PCR. This was unexpected, since the yeast genome does not contain a xylose isomerase gene. This band is, however, not of the correct size.

4.2.2. Growth on xylose of the metabolically engineered base strains

To confirm that the expression of the xylose pathway enables *S. cerevisiae* to grow on xylose as its sole carbon source, the growth of the transformed strain in liquid YNB 4% xylose medium was examined. Yeast transformed with pGREGXKXI was able to grow on minimal media with 4% xylose as its sole carbon source after an extended lag time (96 hrs), reaching an optical density at 600 nm of almost 3, whereas the control strain lacking the plasmid did not grow (Figure 18), confirming that xylose isomerase expression is responsible for this phenotype.

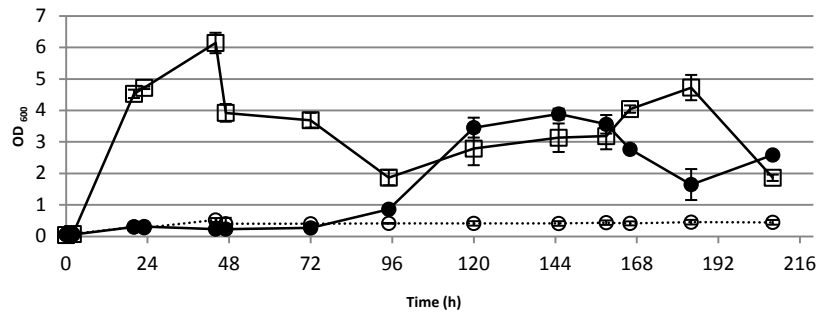


Figure 18. Aerobic growth on minimal media supplemented with 4% xylose of (●) 13d pGREGXXI and (○) the control strain 13d, and of (□) 13d pGREGXXI on minimal medium supplemented with 4% glucose.

Following chromosomal integration of the xylose pathway the $\Delta GRE3 XKXI$ base strains were able to grow on minimal media with 4% xylose as their sole carbon source, with a lag time of about 6 hrs, compared to 96 hrs in the strain carrying the xylose pathway genes on a plasmid. The cultures reached a high optical density of almost 14, at a growth rate of 0.33 h^{-1} (Figure 19), which translates into a biomass yield of at least $0.075 \text{ g g}_{\text{xylose}}^{-1}$, if we assume complete xylose consumption (not measured).

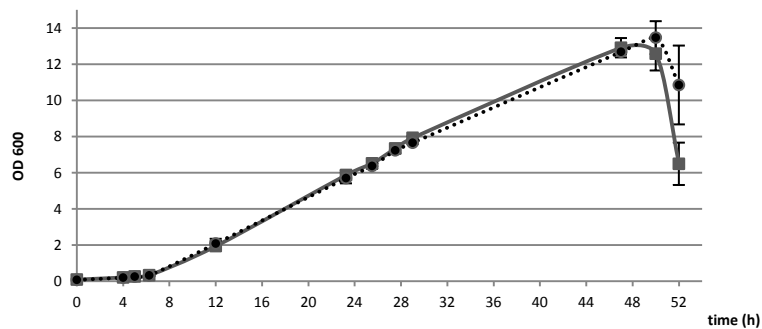


Figure 19. Aerobic growth of base strains 13d $\Delta GRE3XKXI$ (■) and 5d $\Delta GRE3XKXI$ (●) on minimal medium supplemented with 40 g l^{-1} of xylose

4.2.3. Oxygen requirement of the metabolically engineered base strains

In spite of being capable of growth on xylose as the sole carbon source, the $\Delta GRE3$ XKXI strains are unable to ferment xylose to ethanol in anaerobic conditions and require more than 6.3% oxygen in the medium to grow at all (Figure 20).

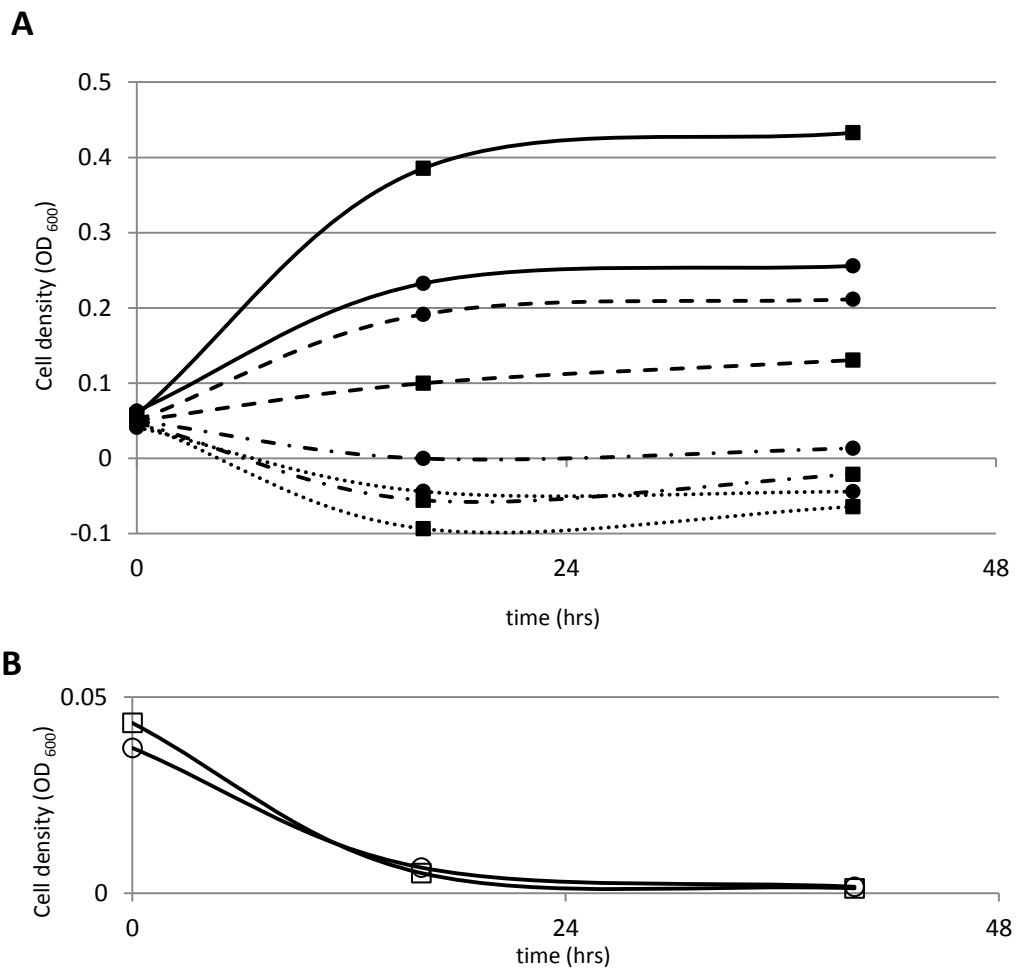


Figure 20. Oxygen dependent growth on xylose of A) 5d $\Delta GRE3$ XKXI (●), 13d $\Delta GRE3$ XKXI (■) in media containing 12.5% (—), 9.4% (---), 6.3% (- · - ·) or 3.1% (····) of oxygen, and B) and control strains 5d $\Delta GRE3$ (○) and 13d $\Delta GRE3$ (□) in xylose medium with a 12.5% oxygen content.

4.3. Mutagenesis

Since the first generation base strains of *S. cerevisiae* engineered for xylose utilization were not capable of anaerobic growth on, or fermentation of xylose, an attempt was made to improve their xylose utilization ability by using UV-mutagenesis to generate a large pool of diverse mutants that could then be selected for improved anaerobic growth on xylose as the sole carbon source. This strategy was selected because of the limited knowledge of the cellular processes that may influence xylose utilization in the engineered strains.

Following irradiation with UV light, YNB plates supplemented with xylose and inoculated with the base strains were incubated both aerobically and anaerobically. For the engineered strains of both mating types aerobically incubated plates yielded more colonies on control plates (not exposed to UV-light) than on irradiated plates, while the trend was reversed in anaerobically incubated plates with more colonies appearing in irradiated plates (Table 1). In aerobic control plates irradiated with 10000 μJ a survival rate of 0.47 was observed after 2 days, 0.72 after 4 days for *MAT α* mutants and 0.51 for *MAT α* mutants after 4 days. On the anaerobically incubated plates of *MAT α* mutants the survival rate was 1.39-fold higher for both irradiation intensities after 5 days compared to the non-irradiated plate (i. e. base strain). For the *MAT α* mutants the survival rate could only be determined after 7 and 8 days. For the plate irradiated with 10000 μJ the survival rate was 31-fold higher after 7 days and 18-fold higher after 8 days compared to the non-irradiated strains, while on plates irradiated with 7500 μJ of UV light survival was 44-fold higher after 7 days and 22-fold higher after 8 days. It should also be noted that

conditions were not completely anoxic due to some leakage in the anaerobic glove chamber caused by a power shut-down, but oxygen levels remained below 0.03% throughout the incubation period, as determined by visual checks of the gas analyzer display at 4 time points spaced equally apart during this 12 hr period.

Table 1. Mutagenesis results: number of colonies on plates irradiated with 10000, 7500 or 0 μ l of UV light and incubated either aerobically or anaerobically.

Strain	UV (μ)	O ₂	2day results	4day results	5day results	7day results	8day results
5D Δ GRE3 XKXI	10,000	-	0	0	6896		
5D Δ GRE3 XKXI	7,500	-	0	0	6928		
5D Δ GRE3 XKXI	0	-	0	0	4976		
5D Δ GRE3 XKXI	10,000	+	~700	2940			
5D Δ GRE3 XKXI	0	+	~1500	4044			
13D Δ GRE3 XKXI	10,000	-	0	0	9	63	92
13D Δ GRE3 XKXI	7,500	-	0	0	48	88	111
13D Δ GRE3 XKXI	0	-	0	0	0	2	5
13D Δ GRE3 XKXI	10,000	+	0	68		74	87
13D Δ GRE3 XKXI	0	+	lawn	133		147	159

This result is consistent with those of other research groups who found that anaerobic growth on xylose was not achievable without some adaptation [51]. All 13824 5d Δ GRE3XKXI colonies and 203 13d Δ GRE3XKXI colonies from the irradiated, anaerobically incubated plates were scraped off and pooled to form the mixed mutant populations that were used in subsequent fermentation experiments.

4.4 Characterization of the mutant strains

4.4.1. Adaptation to oxygen-limited conditions

An attempt was made to improve the growth of these strains in oxygen limited conditions by first subjecting them to UV-mutagenesis and subsequently inoculating them into serial culture of decreasing oxygen content in minimal medium with xylose as the sole carbon source. Results from this experiment (Figure 21) show that the cells did not adapt to limiting oxygen availability, as evidenced by the correlation of the final OD_{600} reached with the oxygen concentration in the culture (Figure 22). The cultures appeared to grow only until all the oxygen was used up (Figure 21), supporting the hypothesis that growth is limited by the amount of electron acceptor available for respiration. Figure 22 shows the correlation between the oxygen concentration in the culture and the final cell density (OD_{600}) reached.

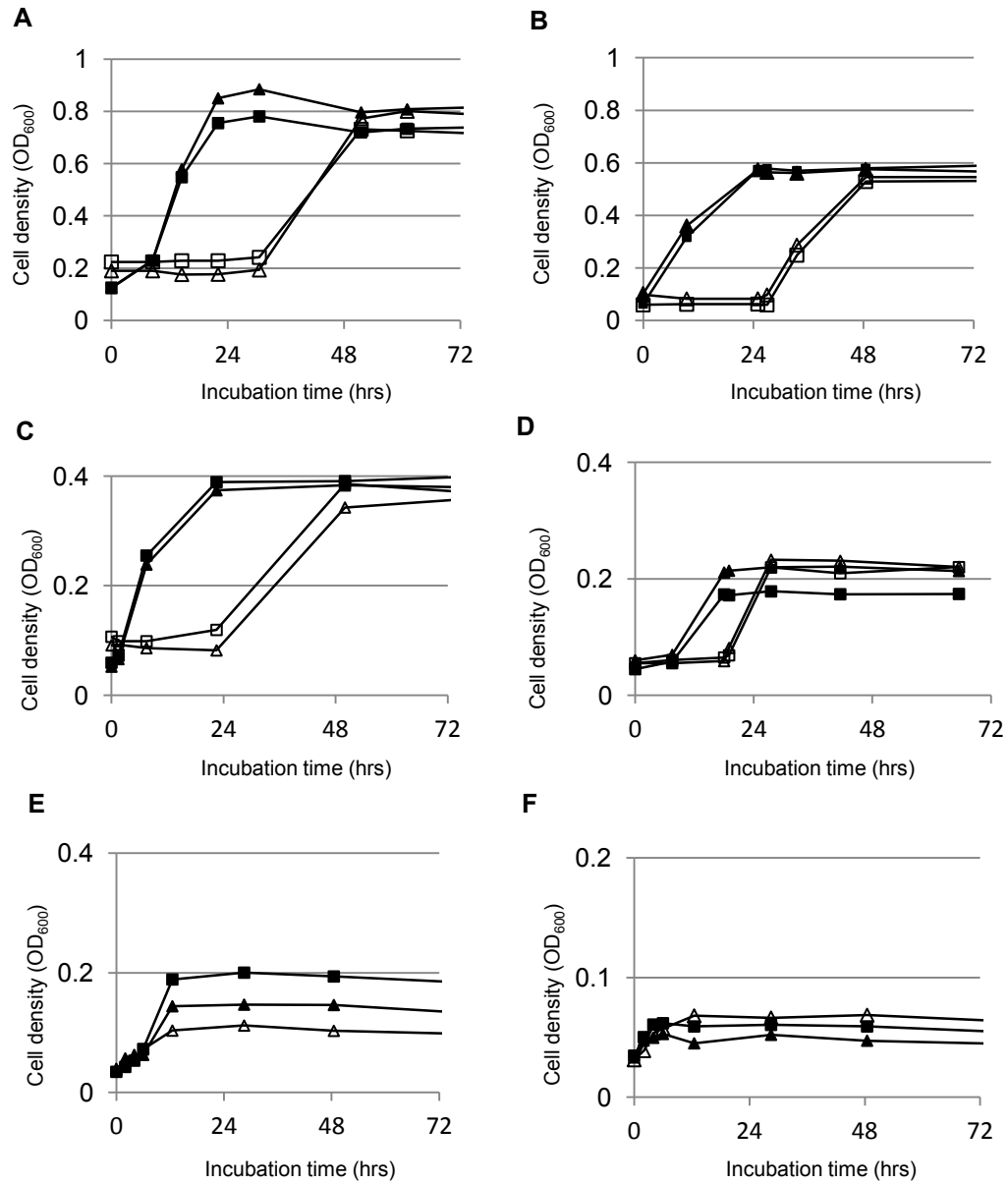


Figure 21. Adaptation to decreasing oxygen availability: growth on xylose of 5dΔGRE3KKXI (□), 13dΔGRE3KKXI (△) and mixed mutant populations 5dΔGRE3KKXI (■) and 13dΔGRE3KKXI (▲) in with A) 9.4%, B) 6.3%, C) 3.1%, D) 1.3%, E) 0.6%, and F) 0% of oxygen available.

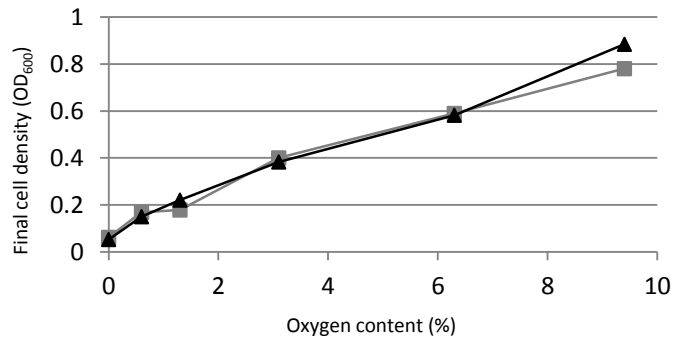


Figure 22. Correlation between the final optical density reached and oxygen availability (%) of mixed mutant populations of 5dΔGRE3XKXI (■) and 13dΔGRE3XKXI (▲)

The mixed mutant cultures did, however, exhibit a decreased lag time relative to the base strain (Figure 21), suggesting that mutagenesis created strains which were more rapidly able to consume xylose. The difference in lag time between mutants and base strains appears to diminish with each transfer into the next culture. The growth profiles suggest that any adaptation by the base strains required for growth in oxygen-limited conditions was maintained in the subsequent culture. While the final cell density was comparable for both mutant and base strains up to an oxygen content of 6.3% in the medium (Figure 21 A,B), at a lower oxygen concentration, a difference begins to be apparent at 3.1% oxygen (Figure 21 C) for the 13d (*MATα*) and at 1.3% oxygen (Figure 21 D) for 5d (*MATα*). At this point, the 5d base control strain was lost due to a sampling needle breaking, allowing for oxygen to enter the bottle. This strain was thus discarded and excluded from subsequent transfers. Nevertheless, at 0% oxygen content in the

medium, both the mutant populations and the 13d base strains behave similarly, exhibiting only negligible growth (Figure 21 F).

4.4.2 Glucose-xylose co-fermentation

From the results of the oxygen-limited growth experiment (Figures 21, 22), it was hypothesised that the strains, while able to grow on xylose aerobically do not recognize it as a fermentable substrate and that inducing fermentation by the presence of glucose might result in the co-fermentation of xylose. To test this hypothesis, glucose-xylose co-fermentation experiments were performed in completely anaerobic conditions.

Mixed mutant populations of both mating types had improved growth in glucose-xylose cultures compared to glucose only cultures (Figure 23). The maximum growth rates reached 0.019 h^{-1} for the *MAT α* and 0.030 h^{-1} for the *MAT α* mixed mutant population, 6.2- and 2.8-fold higher than on glucose alone. Similarly, with xylose in the medium, the mutants reached cell densities 6.0 and 1.6 times higher than without xylose. More biomass is produced from the higher total sugar concentration in the mixed sugar culture, suggesting that xylose is co-utilized with the glucose. In the presence of xylose both the growth rate and the final cell density reached were higher in the mixed mutant populations compared to the *MAT α* base strain. Ethanol production, however, remained below the HPLC detection limit of 0.005% ethanol. The glucose concentration on 0.5% may be limiting for effective ethanolic fermentation to take place. These results show that xylose can be utilized for biomass production by the

mutant populations, but also suggest that they are not able to ferment xylose in anaerobic conditions.

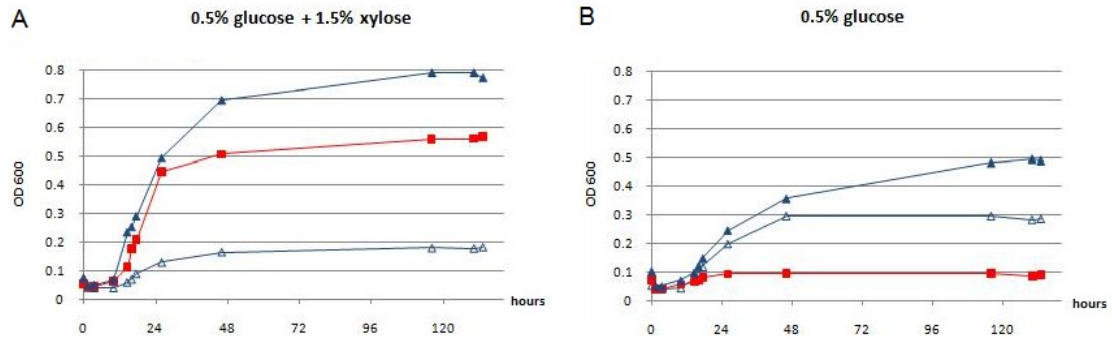


Figure 23. Anaerobic fermentations of mixed mutant populations of *MATα* (▲) and *MATa* (■) and of the *MATα* base strain (△) in minimal media supplemented with A) 0.5% glucose and 1.5% xylose and B) 0.5% glucose alone.

4.4.3. High cell density sugar fermentations

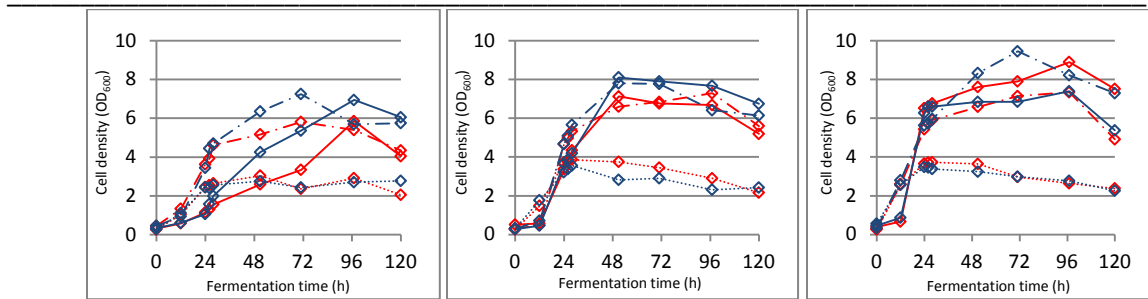
Since xylose can be used by the strains in the presence of glucose but no ethanol production was observed in the low cell density growing cultures, high cell density experiments in micro-aerobic conditions were performed. Both mating types of the base strains, the mixed mutant populations and mutant populations enriched for 80 hrs in YNB xylose medium were grown in three different media: YNB 1.5% xylose, YNB 1.5% xylose + 0.1% glucose or YNB 0.1% glucose. HPLC analysis revealed that both the base strains and the mixed mutant populations were able to ferment xylose to ethanol (Figure 24).

Base strain

Mixed mutant population

Enriched mutant population

A) Growth



B) Substrate and product concentrations

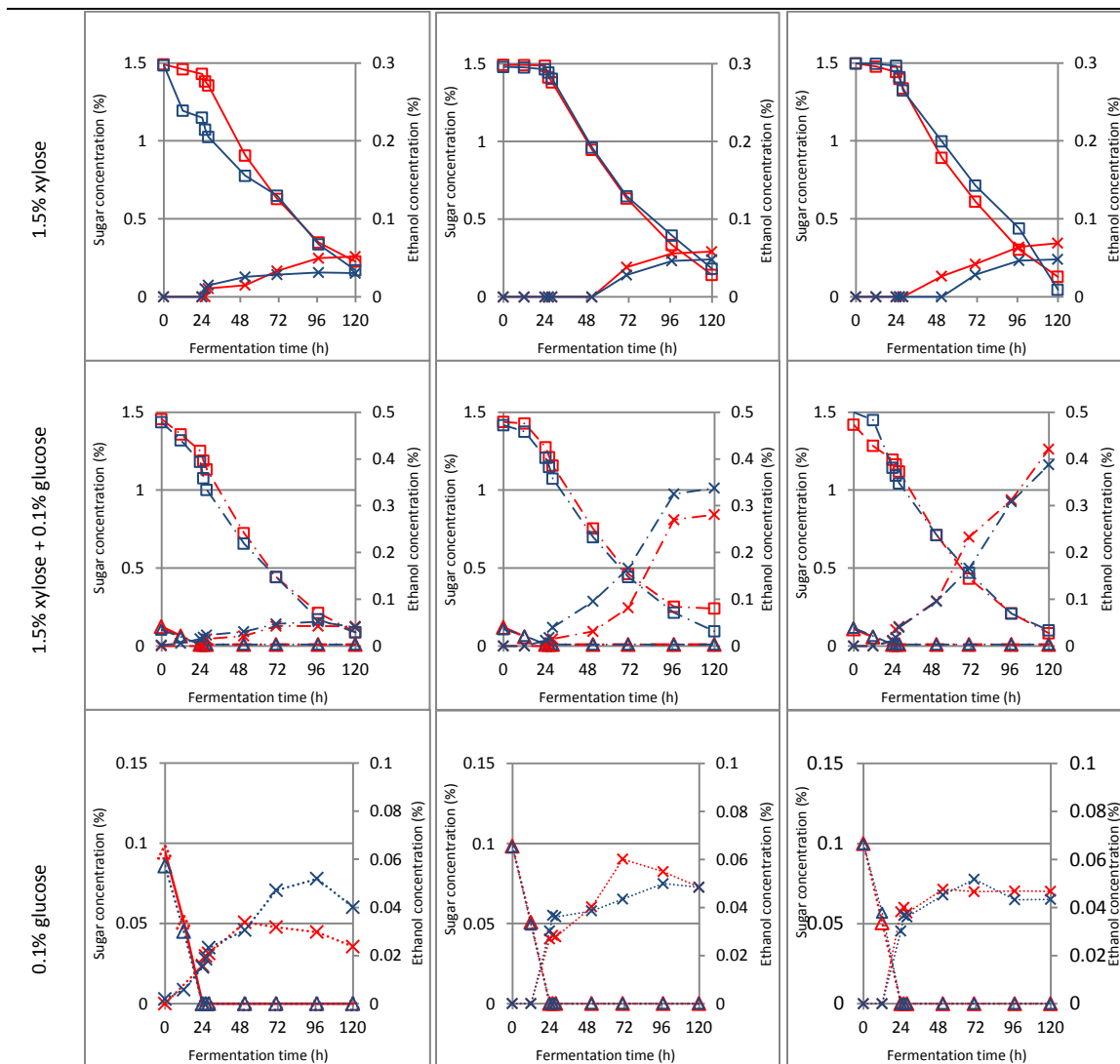


Figure 24: High cell density fermentation. A) growth curves of MAT α (red) and MAT α (blue) base strains, mixed mutant populations and enriched mixed mutant populations grown in minimal media supplemented with 1.5% xylose (—), 1.5% xylose + 0.1% glucose (---), or 0.1% glucose (····); B) xylose consumption (\square), glucose consumption (\triangle), and ethanol production (\times).

The mutant populations exhibited improved growth rates in all media. Ethanol productivities improved in glucose-xylose co-fermentations. Biomass yield improved for the mutant cultures provided with xylose as the sole carbon source, and the estimated ethanol yield from xylose in the co-fermentation cultures also increased. Following enrichment of these mutants, further improvements were observed in the estimated ethanol yield from xylose in the co-fermentations and in the growth rate of cultures grown in xylose-only medium, while ethanol productivities improved slightly in all media.

The high cell density fermentation was repeated twice with the addition of cultures of the enriched mutant populations from the first experiment frozen after 80 hours. Results from the second fermentation are reported here and summarized in Table 2.

Table 2. Summary of results of the high cell density fermentation experiment: fermentation characteristics of the *MAT α* and *MAT α* base strains, mixed mutant populations and enriched mixed mutant populations: the maximum growth rate μ in hour⁻¹, the specific xylose consumption rate r_{xylose} in g xylose g biomass⁻¹ hour⁻¹, biomass yield $Y_{biomass}$ in g biomass g sugar consumed⁻¹, ethanol yield $Y_{ethanol}$ in g ethanol g sugar consumed⁻¹, estimated ethanol yield from xylose in mixed sugar fermentation $Y_{x(ethanol)}$ in g ethanol g xylose consumed⁻¹, specific ethanol productivity $r_{ethanol}$ in g ethanol g biomass⁻¹ hour⁻¹, and the percent ethanol yield % $Y_{ethanol}$ of the maximum ethanol yield of 0.51 g g sugar consumed⁻¹.

Strain		Carbon source	μ	r_{xylose}	$Y_{biomass}$	$Y_{ethanol}$ ($Y_{x(ethanol)}$)	$r_{ethanol}$	% $Y_{ethanol}$
Base	<i>MATα</i>	xylose	0.05	0.0566	0.0076	0.04	0.0015	7.84
		xylose+glucose	0.19	0.0271	0.0019	0.03 (0.01)	0.0009	5.88
		glucose	0.12	-	0.0015	0.25	0.0018	49.02
	<i>MATα</i>	xylose	0.10	0.0271	0.0015	0.02	0.0008	3.92
		xylose+glucose	0.21	0.0234	0.0011	0.04 (0.01)	0.0012	7.84
		glucose	0.06	-	0.0080	0.47	0.0017	92.16
Mutant	<i>MATα</i>	xylose	0.23	0.0226	0.0085	0.04	0.0009	7.84
		xylose+glucose	0.35	0.0231	0.0017	0.21 (0.19)	0.0048	41.18
		glucose	0.19	-	0.0027	0.49	0.0025	96.08
	<i>MATα</i>	xylose	0.26	0.0226	0.0031	0.04	0.0008	7.84
		xylose+glucose	0.33	0.0202	0.0034	0.23 (0.22)	0.0052	45.10
		glucose	0.12	-	0.0003	0.49	0.0026	96.08
Enriched	<i>MATα</i>	xylose	0.48	0.0273	0.0011	0.05	0.0013	9.80
		xylose+glucose	0.24	0.0229	0.0023	0.29 (0.28)	0.0056	56.86
		glucose	0.09	-	0.0061	0.46	0.0035	90.20
	<i>MATα</i>	xylose	0.45	0.0236	0.0102	0.03	0.0009	5.88
		xylose+glucose	0.24	0.0197	0.0024	0.26 (0.25)	0.0055	50.98
		glucose	0.08	-	0.0039	0.44	0.0029	86.27

MAT α base strain (5d Δ GRE3 XKXI)

The MAT α base strain had a specific xylose uptake rate 2.1-fold higher in the absence of glucose (0.0566 g g⁻¹ h⁻¹) than in its presence (0.0271 g g⁻¹ h⁻¹). The specific ethanol productivity is higher in the xylose fermentation at 0.0015 g g⁻¹ h⁻¹, than in the mixed sugar fermentation (0.0009 g g⁻¹ h⁻¹), but lower than the 0.0018 g g⁻¹ h⁻¹ productivity of the glucose fermentation. The higher xylose uptake rate in the xylose fermentation may account for the higher ethanol productivity of this culture.

The growth rate on the other hand is greatest in the co-fermentation at 0.19 h⁻¹, which is 3.8-fold higher than the growth rate of 0.05 h⁻¹ of the xylose fermentation culture and 1.6-fold higher than the rate of 0.12 h⁻¹ of the glucose fermentation culture. In spite of the increased growth rate, the biomass is lower when both sugars are present. While the biomass yield is 1.2-fold higher in the co-fermentation (0.0019 g biomass g⁻¹ sugar consumed) relative to the culture fed only glucose (0.0015 g g⁻¹), the yield is 4 times higher in the xylose fed culture, reaching 0.0076 g g⁻¹. The ethanol yield in the co-fermentation (of 0.03 g ethanol g⁻¹ sugar consumed) on the other hand, is only 75% that attained on xylose alone (0.04 g g⁻¹), perhaps reflecting the 2.1-fold lower xylose uptake rate. The ethanol yield from the glucose-fed culture of 0.25 g g⁻¹ is more than six times the yield on xylose alone and eight times higher than in the co-fermentation. If one assumes that the ethanol produced from glucose fermentation in the co-fermentation culture is equal to the ethanol produced in the glucose-fed culture, then the estimated ethanol yield from the fermentation of the xylose in this culture is

0.01 g g⁻¹. This yield is 25% the yield of the xylose-fed culture, possibly resulting from the 2-fold lower xylose uptake rate in the presence of glucose.

MAT α (13d Δ GRE3XKXI) base strain

The MAT α base strain exhibited similar specific xylose uptake rates in both the xylose (0.0271 g g⁻¹ h⁻¹) and the mixed sugar fermentations (0.0234 g g⁻¹ h⁻¹). While the growth rate was higher in the presence of glucose (0.21 h⁻¹) than in its absence (0.10 h⁻¹) less biomass was produced in the mixed sugar fermentation (0.0011 g g⁻¹) compared to the yield on xylose alone (0.0015 g g⁻¹). The glucose-fed culture had the slowest growth rate of 0.06 h⁻¹, but produced the most biomass at 0.008 g g⁻¹. As was the case for the MAT α base strain, the ethanol yields in xylose-containing media were very low, reaching only 0.02 and 0.04 g g⁻¹ in the absence and presence of glucose, respectively. Assuming equal ethanol yield from glucose in both glucose-containing media, the ethanol yield from xylose of the co-fermentation culture can be calculated to be 0.02 g g⁻¹. This yield is equal to that of the xylose-fed culture, suggesting that the addition of glucose to the medium did not improve the strain's xylose fermentation ability. Unlike MAT α , this strain has an ethanol yield from glucose closer to the theoretical maximum at 0.47 g g⁻¹, suggesting that the MAT α base strain is a healthier strain. Also, in contrast to the MAT α strain, the ethanol productivity is higher in the mixed sugar fermentation (1.2 x 10⁻³ g g⁻¹ h⁻¹) than in the xylose fermentation (8.0 x 10⁻⁴ g g⁻¹ h⁻¹). This result is in accordance with the lower biomass yield and higher ethanol yield in the presence of glucose.

MATa mixed mutant population

The mixed mutant population of the engineered *MATa* strain behaved very differently. Growth rate improved in all media and was again highest in the co-fermentation at 0.35 h^{-1} while the xylose-fed culture and the glucose-fed culture grew at a rate of 0.23 h^{-1} and 0.19 h^{-1} , respectively. The xylose uptake rate in xylose fermentation decreased to $0.0226 \text{ g g}^{-1} \text{ h}^{-1}$, 2.5-fold lower than the base strain, while in the mixed sugar fermentation a similar uptake rate was observed at $0.0231 \text{ g g}^{-1} \text{ h}^{-1}$. While the co-fermentation culture grew faster than the xylose fermentation culture, it produced 5.0 times less biomass (0.0017 g g^{-1}) and 5.0 times more ethanol per gram of sugar consumed (0.21 g g^{-1}). In contrast to the base strain, the estimated ethanol yield from xylose fermentation in the mixed sugar culture is 4.8 times higher than the yield in the xylose fermentation, reaching 0.19 g g^{-1} . Compared to the base strain, for which the yield in the co-fermentation was 25% of the yield of the xylose-fed culture. This result suggests more efficient xylose fermentation by the mutant population in the presence of glucose. Due to the higher ethanol yield and lower biomass yield of the co-fermentation, the specific ethanol productivity is higher than in the xylose fermentation at $0.0048 \text{ g g}^{-1} \text{ h}^{-1}$, which is a 4.3-fold improvement over the base strain. The productivity of the xylose fermentation decreased 1.7-fold to $0.0009 \text{ g g}^{-1} \text{ h}^{-1}$ compared to the base strain, possibly the result of a lower specific xylose uptake rate. These results show increased biomass production from either sugar compared to the base strain, but a decrease when both sugars are utilized. Ethanol yield increased 7-fold in the mixed mutant co-fermentation to 0.21 g g^{-1} , but remained unchanged in the xylose

fermentation. The increase may thus be attributable to the increased amount of ethanol produced from the available glucose, which reaches 96% of the theoretical maximum (0.49 g g^{-1}) in the glucose fermentation. This represents a 2.0-fold increase compared to the base strain. In the glucose fermentation the productivity improved 1.4-fold to $0.0025 \text{ g g}^{-1} \text{ h}^{-1}$.

MAT α mixed mutant population

Mutagenesis of the *MAT α* strain also resulted in improved growth rates in all media and was highest in the co-fermentation at 0.33 h^{-1} compared to 0.12 h^{-1} in the glucose-fed culture and 0.26 h^{-1} in the xylose-fed culture. The xylose uptake rate did not change significantly compared to the base strain and was $0.0226 \text{ g g}^{-1} \text{ h}^{-1}$ for the xylose fermentation and $0.0202 \text{ g g}^{-1} \text{ h}^{-1}$ for the mixed sugar fermentation. The biomass yield is highest when both sugars are utilized (0.0034 g g^{-1}). Slightly less biomass was produced from xylose alone (0.0031 g g^{-1}). These results represent a 3.1- and a 2.1-fold increase for the co-fermentation and the xylose-fermentation relative to the base strain, respectively. The yield from the glucose-fed culture decreased 27-fold to 0.0003 g g^{-1} . Ethanol yields in xylose containing media improved compared to the base strain, at most by a factor of 5.8 in the co-fermentation to 0.23 g g^{-1} , while only slightly from glucose alone to 0.49 g g^{-1} . Similar to the *MAT α* mutants, the estimated ethanol yield from xylose fermentation in the presence of glucose is 5 times higher than the yield in the absence of glucose.

The specific ethanol productivity did not change in the xylose fermentation, but improved slightly (by a factor of 1.1) to $0.0052 \text{ g g}^{-1} \text{ h}^{-1}$ in the mixed sugar fermentation, while in the glucose fermentation it improved 1.6-fold to $0.0026 \text{ g g}^{-1} \text{ h}^{-1}$.

Several trends stand out on the effect of the mutagenesis treatment. Firstly, the growth rate improved for both populations in all media, while the biomass yield increased from xylose fermentation. The ethanol yield increased in all fermentations except for the xylose-fed *MAT α* strain. Notably, the estimated ethanol yield from xylose in the mixed sugar fermentation increased by more than one order of magnitude, suggesting that the presence of glucose aids in xylose fermentation by the mutant populations. The ethanol yield also increased from glucose for the *MAT α* population, but remained unchanged from xylose, while in the *MAT α* population it increased from xylose but only slightly from glucose. One possible explanation for the changes in ethanol yield from glucose alone, is that in the *MAT α* base strain it was extremely low at 0.25 g g^{-1} (49% of the theoretical maximum), while for the *MAT α* base strain it was already at 0.47 g g^{-1} (92%). *MAT α* may simply have had more room for improvement. Mutagenesis also resulted in improved ethanol productivities in the mixed sugar and in the glucose fermentations, but not in the xylose fermentation.

MAT α enriched mutant population

Enrichment of the mutant populations resulted in further improved growth rates in xylose media. For the *MAT α* population the growth rate increased 2.1-fold in the xylose fermentation to 0.48 h^{-1} , but decreased 1.5- and 2.1-fold to 0.24 h^{-1} and 0.09 h^{-1} in the

co-fermentation and glucose fermentation, respectively. The specific xylose uptake rate decreased slightly to $0.0273 \text{ g g}^{-1} \text{ h}^{-1}$ and to $0.0229 \text{ g g}^{-1} \text{ h}^{-1}$ in the absence and in the presence of glucose, respectively. The biomass yield increased in the co-fermentation to 0.0023 g g^{-1} , but this is likely attributable to the increased yield from glucose alone (0.0061 g g^{-1}) since the yield from xylose declined by a factor of 7.7 to 0.0011 g g^{-1} . In xylose-containing media ethanol yield increased 1.3-fold to 0.05 g g^{-1} from xylose alone and 1.4-fold to 0.29 g g^{-1} from both sugars combined, while it decreased slightly from glucose to 0.46 g g^{-1} . The estimated yield from xylose fermentation in the presence of glucose is 5.6 times higher than in its absence at 0.28 g g^{-1} and 1.5 times higher than the yield of the original mutant population. The specific ethanol productivity increased in all media. In both the xylose and the glucose fermentations productivity increased by a factor of 1.4 to $0.0013 \text{ g g}^{-1} \text{ h}^{-1}$ and $0.0035 \text{ g g}^{-1} \text{ h}^{-1}$, respectively. The productivity of the mixed sugar fermentation also increased relative to the original mutant population by a factor of 1.2 to $0.0056 \text{ g g}^{-1} \text{ h}^{-1}$. Enrichment of the mutant population thus resulted in increased ethanol yields and specific ethanol productivities from glucose-xylose co-fermentation.

MAT α enriched mutant population

The enrichment of the *MAT α* mutants resulted in a similar effect on growth rate with a 1.7-fold increase in the xylose fermentation culture to 0.45 h^{-1} , a 1.3-fold increase in the co-fermentation culture to 0.24 h^{-1} and a 1.5-fold increase in the glucose fermentation culture to 0.08 h^{-1} . Increases in the growth rate in xylose containing

media, relative to the mutant population, occurred in spite of similar specific xylose uptake rates. While the ethanol yield was decreased in both single sugar fermentations to 0.03 g g^{-1} from xylose and 0.44 g g^{-1} from glucose, in the xylose-glucose co-fermentation it increased slightly to 0.26 g g^{-1} . The estimated yield from xylose fermentation in the presence of glucose is 8 times higher than in the absence of glucose, suggesting enhanced xylose fermentation in the presence of glucose. The opposite was observed in terms of biomass yield with increases in the single sugar fermentations to 0.0102 g g^{-1} from xylose and 0.0039 g g^{-1} from glucose, but the yield declined in the co-fermentation by a factor of 1.4 to 0.0024 g g^{-1} . The specific ethanol productivity increased slightly (by a factor of 1.1) in all media, reaching $0.0009 \text{ g g}^{-1} \text{ h}^{-1}$ in the xylose fermentation, $0.0029 \text{ g g}^{-1} \text{ h}^{-1}$ in the glucose fermentation, and $0.0055 \text{ g g}^{-1} \text{ h}^{-1}$ in the co-fermentation culture.

The enrichment of the mutant population in xylose media for 80 hrs, resulted in both mating types having improved ethanol yields from total sugar and from xylose alone in the glucose-xylose co-fermentations compared to the mixed mutant populations. Since these cultures exhibited decreased yields from glucose, this increase is likely attributable to an improved xylose fermentation ability in the presence of glucose. In spite of a higher ethanol yield from the glucose fermentation, the co-fermentation cultures exhibited higher specific ethanol productivities.

5. Discussion

In this work I combined metabolic engineering techniques with an evolutionary engineering approach in an attempt to produce a xylose fermenting strain of *S. cerevisiae*. Metabolic engineering is still today the standard for building organisms with improved phenotypes when this can be accomplished by targeting known and relatively simple metabolic networks [72, 73]. This strategy has only limited usefulness when either complex interconnected pathways are targeted or when knowledge of such a pathway is insufficient to allow for targeting of all or most relevant cell processes implicated in the desired phenotype [74]. Evolutionary engineering, on the other hand, can be a powerful tool in producing mutant strains of yeast with a desired phenotype when knowledge of all factors affecting a particular trait is unavailable [75, 76, 77, 78]. It has been known for decades, that *S. cerevisiae* does not possess a functional xylose utilization pathway and efforts have been made to metabolically engineer such a pathway through the expression of exogenous xylose fermentation pathways from bacteria, fungi, and other yeasts [46, 48, 50, 79, 80, 81], but ethanol yields remain low in comparison to glucose fermentation by *S. cerevisiae*. Several research groups have also applied evolutionary engineering techniques in attempts to improve the xylose fermentation ability of metabolically engineered strains and some significant strain improvements have been achieved [51, 54, 61].

Following the construction of a functional xylose utilization pathway through the expression of the exogenous xylose isomerase from *Piromyces* sp. E2 in combination with the deletion of the endogenous xylose reductase and the up-regulation of the

endogenous xylulokinase, my engineered strain was able to grow on xylose aerobically and reverse transcription PCR confirmed the constitutive expression of the xylose isomerase gene. Once the XI-XK construct was integrated into the chromosomes of both mating types, the cultures reached higher cell densities when provided with xylose as the sole carbon source, with a growth rate of 0.33 h^{-1} and a reduced lag time of 6 hours. The improved growth of these strains may be due to more efficient expression of the xylose utilization genes when chromosomally integrated than when expressed from a plasmid. It is also possible that multiple copies of these genes were integrated, given the delta-integration strategy applied in this work, whereas pGREGKXI is a single copy plasmid.

The expression of this pathway did not enable the strains to grow anaerobically on xylose and both the base strains and the mutant populations failed to adapt to decreasing oxygen levels in serial inoculations into media of decreasing oxygen concentration (Figure 21). When the media were supplemented with glucose in addition to xylose, both the growth rate and final cell density reached by the mutant strains were higher than when no xylose was available (Figure 23), suggesting that in the presence of glucose they are able to co-utilize xylose. The low sugar concentration of 0.5% may also be limiting anaerobic growth.

While our yields from high cell density fermentations were generally lower than those reported by other groups, media composition is likely to have played a significant role in these results. Other researchers used either rich medium supplemented with xylose and sometimes glucose as well, or they supplemented minimal medium with

ergosterols, vitamins, and/or minerals in addition to the carbon source. In the fermentation results presented here YNB was supplemented only with a carbon source. In an industrial setting, the added cost of supplementing hydrolysates is undesirable, hence, I believe that the xylose fermentation should be optimized without costly supplementation.

While the base strains in this study were able to grow fermentatively in micro-aerobic conditions on both xylose and a xylose-glucose mixture, ethanol yields were below 15% of the theoretical maximum ethanol yield from xylose (Tables 2). Surprisingly the ethanol yield was also low for the *MATa* base strain in the glucose fermentation, perhaps due to the increased metabolic burden of constitutive expression of the novel xylose metabolic pathway. Introducing mutations by UV exposure generated mutants with improved growth rates in all media, as well as improved ethanol yield and specific productivity from glucose-xylose co-fermentations. Accelerated evolution through the generation of mutations at a higher rate than they would naturally occur is, therefore, a powerful strategy for the rapid improvement of these phenotypes.

While enrichment of the mixed mutant populations (Table 2) resulted in increased growth rates on xylose as the sole carbon source, the ethanol yield from xylose fermentation remained lower than the yield from glucose fermentation. Therefore, further improvement of the strains is required to produce efficient xylose-fermenting strains of *S. cerevisiae*. The yield from xylose in the mixed sugar fermentation is, however, six and eight times higher than the yield in the xylose fermentation. On a per gram of cells basis, ethanol production is faster in the presence of both sugars than in

glucose-fed cultures. Together, these results suggest that glucose fermentation enhances the strain's ability to ferment xylose.

The best results from fermentations reported in this work in terms of the ethanol yield attained are 0.29 and 0.26 g g⁻¹ (57 and 51 % of theoretical maximum) in the glucose-xylose co-fermentations of the enriched mutant populations for *MATα* and *MATα*, respectively (Table 2). These results are comparable to those reported by Zaldivar [55] of 0.23 g g⁻¹ (45% of theoretical maximum) for strain TMB 3001, which expresses a xylose reductase and a xylitol dehydrogenase from *Pichia stipitis* as well as the endogenous xylulose reductase under constitutive promoters. Our growth rates of 0.24 h⁻¹ for both mating types are also comparable to those achieved by this group of 0.26 h⁻¹. Zaldivar supplemented minimal media with 50 g l⁻¹ glucose and 50 g l⁻¹ xylose, as well as with trace metal and vitamin solutions as well as ergosterols and performed fermentation in completely anaerobic conditions. Eliasson [50] achieved ethanol yields of 0.34 g g⁻¹ (67% of theoretical maximum) for TMB 3001 fed 15 g l⁻¹ of xylose plus 5 g l⁻¹ of glucose, only 1.2-1.3-fold higher than the results presented here. In this study minimal medium was supplemented with ergosterols as well. Application of evolutionary engineering techniques of random mutagenesis and adaptation to growth on xylose as the sole carbon source on this strain produced TMB 3001-C1, which produced 0.24 g g⁻¹ ethanol (47% of theoretical maximum) in micro-aerobic fermentation of 10 g l⁻¹ of xylose [53]. Zaldivar also expressed the same pathway in an industrial yeast strain producing strain A4, which in glucose-xylose co-fermentations (30 g l⁻¹ of each sugar) exhibited a higher xylose uptake rate (0.21 g g⁻¹ h⁻¹), but an ethanol

productivity similar to TMB 3001 at $0.04 \text{ g g}^{-1} \text{ h}^{-1}$. Ethanol yield was 1.2-fold higher at 0.27 g g^{-1} (53% of theoretical maximum).

Wahlboom's group [51] expressed the same three genes from the yeast chromosome and reported a specific xylose uptake rate of $0.065 \text{ g g}^{-1} \text{ h}^{-1}$ of the resulting strain (TMB 3399) when grown aerobically with xylose as the sole carbon source. Compared to the uptake rate (0.056 and $0.027 \text{ g g}^{-1} \text{ h}^{-1}$) of the base strains presented in this work, this value is 1.2 and 2.4 times higher, however, the values were calculated from micro-aerobic fermentations, whereas Wahlboom's group did not report the value for their micro-aerobic fermentation. Similar to these results, no ethanol was detected during aerobic growth. In micro-aerobic conditions Wahlboom's group achieved an ethanol yield of 0.21 g g^{-1} and an ethanol productivity of $0.001 \text{ g g}^{-1} \text{ h}^{-1}$. While the yields of the base strains reported here were an order of magnitude lower, the productivity was comparable in the *MAT α* base strain, but 1.25 times higher for *MAT α* . Following random mutagenesis and xylose adaptation they achieved a 1.2-fold improvement in ethanol yield to 0.25 g g^{-1} and a 100-fold increase in productivity to $0.1 \text{ g g}^{-1} \text{ h}^{-1}$ by strain TMB 4000 [51]. Similarly, in this work, mutagenesis followed by enrichment in xylose media produced a 1.5-fold increase in ethanol yield for *MAT α* and a 1.25-fold increase for *MAT α* , compared to the base strains. Ethanol productivities changed only slightly, with a 1.1-fold higher productivity for *MAT α* , but a 1.1-fold lower productivity for *MAT α* .

Matsushika and his group attempted to circumvent the redox imbalance problems generated by the expression of the yeast pentose fermentation pathway in *S. cerevisiae* by expressing a xylitol dehydrogenase modified to prefer NADP^+ as a co-factor, in

addition to expressing the xylose reductase from *Pichia stipitis* and the endogenous xylulokinase [52]. In anaerobic fermentations of 45 g l⁻¹ of xylose, strain MA-N5 produced 0.36 g g⁻¹ of ethanol. The most significant improvement over MA-N4 (control strain expressing the wild-type xylitol dehydrogenase) was 1.5-fold higher ethanol productivity to 0.09 g g⁻¹ h⁻¹. Their mutation also resulted in a 1.3-fold increase in xylose uptake to 0.25 g g⁻¹ h⁻¹. Bengtsson [82] also expressed a mutated xylitol dehydrogenase for NADP⁺ preference in conjunction with a xylose reductase, xylulokinase and up-regulating enzymes of the non-oxidative pentose phosphate pathway producing TMB 3200. In anaerobic glucose-xylose co-fermentations with 10 g l⁻¹ of each sugar this strain produced 0.39 g ethanol per g of sugar with a specific productivity of 0.51 g g⁻¹ h⁻¹ and specific xylose uptake rate of 0.28 g g⁻¹ h⁻¹. The highest ethanol yields produced by the evolved strains here are 1.3-1.5 times lower (*MAT α* and *MAT α* , respectively) in mixed sugar fermentation, which may be attributable to the higher concentration of glucose used by Bengtsson's group. More significantly, the specific xylose uptake rate and ethanol productivity shown by Bengtsson *et al.* are one and two orders of magnitude higher than those shown here, possibly the result of the increased flux of xylose metabolites through the pentose phosphate pathway genes to increase flux.

Wisselink's group also expressed the *Pichia stipitis* xylose reductase and xylitol dehydrogenase in a different strain of *S. cerevisiae* producing strain IMS0003 [83]. This strain achieved a high ethanol yield 0.44 g g⁻¹ (86% of theoretical maximum) in anaerobic co-fermentations with 15 g l⁻¹ xylose, 15 g l⁻¹ arabinose and 30 g l⁻¹ glucose. Following xylose adaptation, the resulting strain IMS0007 improved 1.5-fold in xylose

uptake. Further improvements in xylose uptake were achieved by IMS0010, the evolved strain after consecutive batch cultivations, with $0.35 \text{ g g}^{-1} \text{ h}^{-1}$, while the ethanol yield remained unchanged in IMS0007, but declined slightly to 0.43 g g^{-1} in IMS0010. The high ethanol yield (1.5 and 1.7-fold higher relative to enriched *MAT α* and *MAT α* , respectively) compared to the strains described here may, however, be the result of the up-regulation of pentose phosphate pathway genes *TKL1*, *TAL1*, *RPE1* and *RKI1*.

Various bacterial xylose isomerases have been expressed in *S. cerevisiae*. In 2005, Karhumaa expressed one from *Thermus thermophilus* in conjunction with the deletion of *GRE3* and the expression of exogenous *TKL1* and *TAL1*, as well as xylose adaptation [84]. In micro-aerobic fermentations of 50 g l^{-1} xylose, the resulting strain TMB 3050 produced 0.29 g g^{-1} of ethanol with a low xylose uptake rate of $0.002 \text{ g g}^{-1} \text{ h}^{-1}$. In spite of the low xylose uptake, the ethanol yield was 56% of the theoretical maximum. Considering that the specific xylose uptake rate of the mutated and evolved strains in this work is an order of magnitude higher but the ethanol yields are 5.8 and 9.7 times lower (for *MAT α* and *MAT α* xylose fermentation, respectively), the uptake of xylose may not be the limiting factor in efficient xylose fermentation of these strains, but improving the flux of xylose towards the pentose phosphate pathway may be of greater importance.

When in 2007 the same group expressed the xylose isomerase of *Piromyces* sp. E2 instead of the *T. thermophilus* (in conjunction with *GRE3* deletion, xylulokinase up-regulation and the expression of *TAL1*, *TKL1*, *RKI1*, and *RPE1*), the resulting strain TMB 3066 had a higher specific xylose uptake rate ($0.05 \text{ g g}^{-1} \text{ h}^{-1}$) and ethanol yield (0.43 g g^{-1})

[85]. In their work, the authors compared TMB 3066 to TMB 3057, which are similar strains that express the *Pichia stipitis* xylose reductase and xylitol dehydrogenase instead of a xylose isomerase. While TMB 3057 displayed 2.6 times higher xylose uptake rate at $0.13 \text{ g g}^{-1} \text{ h}^{-1}$ and double the ethanol productivity at $0.04 \text{ g g}^{-1} \text{ h}^{-1}$ ($0.02 \text{ g g}^{-1} \text{ h}^{-1}$ for TMB 3066), the ethanol yield was 1.3-fold lower, suggesting that the eukaryotic xylose isomerase pathway is superior to the xylose reductase/xylitol dehydrogenase pathway in the rate of xylose consumption and ethanol production, but inferior in terms of using xylose to produce ethanol.

Strain MT8-1/XK δ XI [86] expressing a xylose isomerase from *Orpinomyces* sp. exhibited an ethanol yield of 0.32 g g^{-1} and a specific xylose uptake rate of $0.019 \text{ g g}^{-1} \text{ h}^{-1}$ in fermentations of both 30 g l^{-1} of xylose, and 30 g l^{-1} of both xylose and glucose. The specific ethanol productivity was 2.3-times higher in the presence of glucose at $0.014 \text{ g g}^{-1} \text{ h}^{-1}$. Deleting the *GRE3* gene resulted in a more than 2-fold increase in the specific xylose uptake rate to $0.039 \text{ g g}^{-1} \text{ h}^{-1}$ in micro-aerobic xylose fermentation and to $0.042 \text{ g g}^{-1} \text{ h}^{-1}$ in mixed-sugar fermentation. The deletion also resulted in a 1.1-fold increase in ethanol yield to 0.32 and 0.34 g g^{-1} , in xylose and in glucose-xylose fermentation, respectively. The specific ethanol productivity increased 2.3-fold to $0.0140 \text{ g g}^{-1} \text{ h}^{-1}$ in xylose and 2.0-fold to $0.0280 \text{ g g}^{-1} \text{ h}^{-1}$ in glucose-xylose fermentations [86]. Comparing MT8-1 Δ GRE3/XK δ XI, in xylose fermentation the enriched mutant strains described here produced about an order of magnitude less ethanol per gram of xylose consumed at a rate also about one order of magnitude slower, in spite of only a slightly lower xylose uptake rate (1.4 and 1.6-fold lower for *MAT α* and *MAT α* , respectively). In the mixed

sugar fermentation, xylose uptake rates were about 2-fold lower at $0.023 \text{ g g}^{-1} \text{ h}^{-1}$ for *MATa* and $0.020 \text{ g g}^{-1} \text{ h}^{-1}$ for *MAT α* . In spite of an increased difference in specific xylose uptake between our strain compared to the difference in the xylose fermentation, the difference in ethanol yield and productivity is decreased, and these strains produce 1.2 and 1.3 times less ethanol with yields of 0.29 g g^{-1} and 0.26 g g^{-1} and five times lower ethanol productivities at $0.0056 \text{ g g}^{-1} \text{ h}^{-1}$ and $0.0055 \text{ g g}^{-1} \text{ h}^{-1}$ for *MATa* and for *MAT α* , respectively. His yields and productivities from total sugar in the co-fermentation may reflect the lower xylose to glucose ratio used by Tanino's group (30 g l^{-1} of both sugars) compared to my work (5 g l^{-1} of glucose and 15 g l^{-1} of xylose)

In 2003 the Kuyper group was the first to attempt expressing the *Piromyces* sp. E2 xylose isomerase in *S. cerevisiae* on a plasmid. The resulting strain RWB 202 achieved ethanol yields of 0.39 g g^{-1} (76% of theoretical maximum) in oxygen-limited fermentations on minimal media supplemented only with a carbon source (10 g l^{-1} of xylose plus 20 g l^{-1} of glucose) [58]. This yield is also comparable to the ones achieved in this study (1.3-1.5 times higher), as the difference may be attributable to the much higher glucose to xylose ratio employed by Kuyper's group. One year later the same group reported a spontaneous mutant (RWB 202-AFX) with an improved ethanol yield of 0.42 g g^{-1} (82% of theoretical maximum) on minimal media supplemented with 20 g l^{-1} of xylose and ergosterols [59]. When this group also up-regulated the endogenous xylulokinase as well as various glycolytic enzymes and deleted the aldose reductase encoding *GRE3*, the resulting strain RWB 217 was able to produce 0.43 grams of ethanol per gram of sugar consumed (84% of theoretical maximum) [60]. Following evolutionary

engineering of RWB 217, RWB 218 had a similar ethanol yield of 0.40 g g^{-1} in medium supplemented with 2% glucose and 2% xylose, as well as an equal growth rate of 0.25 h^{-1} , but biomass yield increased from 0.074 to 0.084 g g^{-1} . In fermentation with xylose as the only carbon source, however, RWB 218 performed better than RWB 217, with a 1.3-fold increase in growth rate, a 1.2-fold increase in biomass yield, but a 1.05-fold decrease in ethanol yield [61]. Compared to strains reported here, in 1.5% xylose and 0.1% glucose a growth rate of 0.24 h^{-1} but a much lower biomass yield of 0.002 g g^{-1} was observed.

A direct comparison of results across such differently designed studies is impossible. Synthetic media are inadequate to predict the behaviour of strains engineered in a laboratory once they are transferred to an industrial setting. While it is a necessary starting point, the performance of strains in such controlled conditions does not necessarily translate to industrial processes in the fermentation of biomass hydrolysates.

The current performance of the strains described here, is not necessarily the end-point of evolutionary engineering and further improvements are likely achievable through the application of other strain improvement techniques. The specific xylose uptake rates remain significantly lower than those achieved by other researchers [51, 52, 53, 55, 59, 60, 61, 82, 83, 85]. The ethanol yield remains below 60% of the theoretical maximum, which is still much lower than the 82-86% reported yields of other recombinant *S. cerevisiae* strains [52, 60, 83, 85]. Since ethanol was the only end-product measured in this study, we cannot attest to the fates of the sugars consumed.

In spite of the deletion of the xylose reductase encoding *GRE3* gene, xylitol could still be produced either from xylulose by the action of the xylitol dehydrogenase, which catalyzes the reversible conversion of xylitol and xylulose, or from xylose by the action of aldose reductases other than the deleted xylose reductase.

To further improve the fermentation profile of our strains other evolutionary engineering techniques may prove to be valuable. The two mutant populations are likely to carry different mutations which when recombined through mating could result in improved fermentation abilities by the synergistic action of two beneficial mutations. The combination of silent mutations with each other or with a beneficial one may also result in an improved phenotype, as could the removal of a deleterious one. Due to our lack of knowledge of all the factors that could potentially contribute to an efficient xylose fermentation phenotype, techniques such as these are likely to speed up the process of developing the ideal strain of yeast for the fermentation of biomass hydrolysates.

Table 3: Performance of metabolically-engineered and xylose-adapted strains of *S. cerevisiae* in fermentation experiments.

Strain	Description	Aeration	Xylose (g L ⁻¹)	Glucose (g L ⁻¹)	r_{xylose} (g g ⁻¹ h ⁻¹)	$Y_{ethanol}$ (g g ⁻¹)	$r_{ethanol}$ (g g ⁻¹ h ⁻¹)	References
TMB 3001	XR, XDH, XK	AN	0	20	NS	0.30	NS	[50]
		AN	5	15	NS	0.30	NS	"
		AN	10	10	NS	0.29	NS	"
		AN	5	15	NS	0.26	NS	"
TMB 3001	XR, XDH, XK	AN	50	50	0.060	0.23	0.0400	[55]
A4	XR, XDH, XK	AN	50	50	0.210	0.27	0.0400	"
TMB 3001 C1	TMB 3001 + random mutagenesis and xylose adaptation	AN	10	0	NS	0.24	NS	[53]
TMB 3399	XR, XDH, XK	AE	20	0	0.065	0.00	NS	[51]
		MA	20	0	NS	0.21	0.0010	"
		AN	20	0	NS	0.05	0.0006	"
TMB 4000	TMB 3399 + mutagenesis and xylose adaptation	AE	20	0	0.350	0.00	NS	"
		MA	20	0	NS	0.25	0.1000	"
		AN	20	0	NS	0.18	0.0240	"
RWB 202	XI (from <i>Piromyces</i> sp. E2)	AN	10	20	NS	0.39	NS	[58]
RWB 202-AFX	RWB 202 + xylose adaptation	AN	20	0	0.340	0.42	0.1400	[59]
RWB 217	XI, XK, Δ GRE3, TAL, TKL, RPE, RKI	AN	20	0	1.060	0.43	0.4900	[60]
		A	20	20	NS	0.43	NS	"
RWB 218	RWB 217 + xylose adaptation	AN	20	0	0.900	0.41	NS	[61]
		AN	20	20	NS	0.40	NS	"
		AN	100	25	NS	0.38	NS	"
TMB 3050	Δ GRE3, XI (from <i>Thermus thermophilus</i>), TAL1 TKL + xylose adaptation	MA	50	0	0.002	0.29	NS	[84]
TMB 3057	Δ GRE3, XR, XDH, XK, TAL, TKL, RKI, RPE	AN	50	0	0.130	0.33	0.0400	[85]
TMB 3066	Δ GRE3, XI (from <i>Piromyces</i> sp. E2), XKS, TAL, TKL, RKI, RPE	AN	50	0	0.050	0.43	0.0200	"
BP000	XR (from <i>Candida tenuis</i>)	MA	20	0	0.070	0.24	NS	[56]
"		AN	20	0	0.060	0.24	NS	"
BP10001	XR (from <i>Candida tenuis</i> mutated for NADH preference)	MA	20	0	0.070	0.34	NS	"
"		AN	20	0	0.080	0.34	NS	"
MA-N4	XR, XDH (wt), XK	AN	45	0	0.190	0.34	0.0600	[52]
MA-N5	XR, XDH (mutated for NADP preference), XK	AN	45	0	0.250	0.36	0.0900	"
MA-R4	XR, XDH, XK	AN	45	0	NS	0.35	0.0075	"
		AN	45	45	NS	0.42	NS	"

Table 3 (continued)

Strain	Description	Aeration	Xylose (g L ⁻¹)	Glucose (g L ⁻¹)	r_{xylose} (g g ⁻¹ h ⁻¹)	$Y_{ethanol}$ (g g ⁻¹)	$r_{ethanol}$ (g g ⁻¹ h ⁻¹)	Reference
IMS0003	XR, XDH	AN	15	30	0.210	0.44	NS	[83]
IMS0007	IMS0003 + xylose adaptation	AN	15	30	0.310	0.44	NS	“
IMS0010	Single colony isolated from consecutive batch cultivation	AN	15	30	0.350	0.43	NS	“
TMB 3200	XDH(mutated for NADP preference), XR, XK, ↑n.o.PPP	AN	10	10	0.280	0.39	0.5100	[82]
BP000	XR (from <i>Candida tenuis</i>)	AN	10	10	0.050	0.23	NS	[87]
BP10001	XR (from <i>Candida tenuis</i> mutated for NADH preference)	AN	10	10	0.050	0.30	NS	“
MT8-1/XKΔXI	XI (from <i>Orpinomyces</i> sp.), XK	MA	30	0	0.019	0.32	0.0060	[86]
		MA	30	30	0.019	0.32	0.0140	“
MT8-1ΔGRE3/XKΔXI	XI (from <i>Orpinomyces</i> sp.), XK, ΔGRE3	MA	30	0	0.039	0.35	0.0140	“
		MA	30	30	0.042	0.34	0.0280	“

Abbreviations:

Strain description: wt – wild type; ↑n.o. PPP – up-regulation of non-oxidative pentose phosphate pathway genes

Aeration: AN – anaerobic; AE – aerobic; MA – micro-aerobic

r_{xylose} – specific xylose uptake rate; $Y_{ethanol}$ – ethanol yield; $r_{ethanol}$ – specific ethanol productivity.

6. References

1. Stein, K., *Food vs Biofuel*. Journal of the American Dietetic Association, 2007. **107**: 1870-1878.
2. Tokgoz, *Emerging Biofuels: Outlook of effects on U.S. grain, oilseed, and livestock markets*. Staff report 07-SR 101, Center for Agricultural and Rural Development, Iowa State University, 2007.
3. Hill, J., E. Nelson, D. Tilman, S. Polasky, D. Tiffany, *Environmental, economic, and energetic costs and benefits of biodiesel and ethanol biofuels*. PNAS, 2006. **103**: 11206-11210.
4. Hertel, T.W., W. E. Tyner, D. K. Birur, *Biofuelsforall? Understanding the global impacts of multinational mandates*, Center for Global Trade Analysis, Department of Agricultural Economics, Purdue University, 2008. GTAP Working Paper No.51, 48pp.
5. Fargione, J., J. Hill, D. Tilman, S. Polasky, P. Hawthorne, *Land clearing and the biofuel carbon debt*. Science, 2008. **319**: 1235-1237.
6. Lynd, L. R., C. E. Wyman, T. U. Gerngross, *Biocommodity engineering*. Biotechnol. Prog., 1999. **15**: 777-793.
7. Nilverbrant N. O., and P. Persson, *Limits for alkaline detoxification of dilute acid lignocelluloses hydrolysates*. Applied Biochemistry and Biotechnology, 2003. **107**: 615-628.
8. van Maris, A. J., D. A. Abbott, E. Bellissimi, J. van den Brink, M. Kuyper, M. A. Luttik, H. W. Wisselink, W. A. Scheffers, J. P. van Dijken, and J. T. Pronk, *Alcoholic fermentation of carbon sources in biomass hydrolysates by Saccharomyces cerevisiae: current status*. Antonie van Leeuwenhoek, 2006. **90**: 391-418.
9. Wiegel J., and L.G. Ljungdahl, *The importance of thermophilic bacteria in biotechnology*. Critical Reviews in Biotechnology, 1986. **3**: 39-108.
10. Laci, L. S., H.G. Lawford, *Thermoanaerobacter ethanolicus in a comparison of the growth efficiencies of thermophilic and mesophilic anaerobes*. Journal of Bacteriology, 1985. **163**: 1275-1278.

11. Sommer, P., T. Georgieva, and B. K. Ahring, *Potential for using thermophilic anaerobic bacteria for bioethanol production from hemicelluloses*. Biochemical Society Transactions, 2004. **32**: 283-289.
12. Ahring, B. K., K. Jensen, P. Nielsen, AB Bjerre, *Pretreatment of wheat straw and conversion of xylose and xylan to ethanol by thermophilic anaerobic bacteria*. Bioresource Technology, 1996. **58(2)**: 107-113.
13. Laci, L. S. and H. G. Lawford, *Thermoanaerobacter ethanolicus growth and product yield from elevated levels of xylose or glucose in continuous cultures*. Applied and Environmental Microbiology, 1991. **57**: 579-585.
14. Dien, B. S., M. A. Cotta, and T. W. Jeffries, *Bacteria engineered for fuel ethanol production: current status*. Applied Microbiology and Biotechnology, 2003. **63**: 258-266.
15. Ingram, L. O., T. Conway, D. P. Clark, G. W. Sewell, and J. F. Preston, *Genetic engineering of ethanol production in Escherichia coli*. Applied and Environmental Microbiology, 1987. **53**: 2420-2425.
16. Ohta, K., D. S. Beall, J. P. Mejia, K. T. Shanmugam, and L. O. Ingram, *Genetic improvement of Escherichia coli for ethanol production: chromosomal integration of Zymomonas mobilis genes encoding pyruvate decarboxylase and alcohol dehydrogenase II*. Applied and Environmental Microbiology, 1991. **57**: 893-900.
17. Hespell, R. B., H. Wyckoff, B. S. Dien, and R. J. Bothast, *Stabilization of pet operon plasmids and ethanol production in Escherichia coli strains lacking lactate dehydrogenase and pyruvate formate-lyase activities*. Applied and Environmental Microbiology, 1996. **62**: 4594-4597.
18. Dien, B. S., R. B. Hespell, H. A. Wyckoff, and R. J. Bothast, *Fermentation of hexose and pentose sugars using a novel ethanologenic Escherichia coli strain*. Enzyme and Microbial Technology, 1998. **23**: 366-371.
19. Rogers, P. L., K. J. Lee, M. L. Skotnicki, and D. E. Tribe, *Ethanol production by Zymomonas mobilis*. Advances in Biochemical Engineering/ Biotechnology, 1982. **23**: 37-84.

20. Zhang, M., C. Eddy, K. Deanda, M. Finkelstein, and S. Picataggio, *Metabolic engineering of a pentose metabolism pathway in ethanologenic Zymomonas mobilis*. *Science*, 1995. **267**: 240-243.
21. Joachimsthal, E. L., and P. L. Rogers, *Characterization of a high-productivity recombinant strain of Zymomonas mobilis for ethanol production from glucose/xylose mixtures*. *Applied Biochemistry and Biotechnology*, 2000. **84-86**: 343-356.
22. Lawford, H. G., and J. D. Rousseau, *Performance testing of Zymomonas mobilis metabolically engineered for cofermentation of glucose, xylose, and arabinose*. *Applied Biochemistry and Biotechnology*, 2002. **98-100**: 429-448.
23. Mohagheghi, A., K. Evans, Y.-C. Chou, and M. Zhang, *Cofermentation of glucose, xylose, and arabinose by genomic DNA-integrated xylose/arabinose fermenting strain of Zymomonas mobilis*. *Applied Biochemistry and Biotechnology*, 2002. **98-100**: 885-898.
24. Kim, I. S., K. D. Barrow, and P. L. Rogers, *Nuclear magnetic resonance studies of acetic acid inhibition of Rec Zymomonas mobilis ZM4 (pZB5)*. *Applied Biochemistry and Biotechnology*, 2000. **84-86**: 357-370.
25. Skoog, K., and B. Hahn-Hägerdal, *Xylose fermentation*. *Enzyme and Microbial Technology*, 1988. **10**:66-80.
26. Hahn-Hägerdal, B., H. Jeppson, L. Olsson, and A. Mohagheghi, *An interlaboratory comparison of the performance of ethanol-producing microorganisms in a xylose-rich acid hydrolysate*. *Applied Microbiology and Biotechnology*, 1994. **41**: 62-72.
27. Chiang, C., and S. G. Knight, *Metabolism of D-xylose by moulds*. *Nature*, 1960. **188**: 79-81.
28. Harhangi, H. R., A. S. Akhmanova, R. Emmens, C. van der Drift, W. T. de Laat, J. P. van Dijken, M. S. Jetten, and J. T. Pronk, H.J. Op den Camp, *Xylose metabolism in the anaerobic fungus Piromyces sp. E2 follows the bacterial pathway*. *Archives in Microbiology*, 2003. **180**: 134-141.

29. Gunsalus, I. C., B. L. Horecker, and W. A. Wood, *Pathways of carbohydrate metabolism in microorganisms*. Bacteriology Reviews, 1955. **19**: 79-128.
30. Toivola, A., D. Yarrow, E. van den Bosch, J. P. van Dijken and W. A. Scheffers, *Alcoholic fermentation of D-xylose by yeasts*. Applied and Environmental Microbiology, 1984. **47**: 1221-1223.
31. Barnett, Yeast characteristics and identification. Cambridge University Press, 2000. Cambridge.
32. McMillan, J. D., and B. L. Boynton, *Arabinose utilization by xylose-fermenting yeasts and fungi*. Applied Biochemistry and Biotechnology, 1994. **45-46**: 569-584.
33. Dien, B. S., C. P. Kurtzman, B. C. Saha, and R. J. Bothast, *Screening for L- arabinose fermenting yeasts*. Applied Biochemistry and Biotechnology, 1996. **57-58**: 233-242.
34. Skoog, K., and B. Hahn-Hägerdal, *Effects of oxygenation on xylose fermentation by Pichia stipitis*. Applied and Environmental Biotechnology, 1990. **56**: 3389-3394.
35. Fonseca, C., I. Spencer-Martin, and B. Hahn-Hägerdal, *L-Arabinose metabolism in Candida arabinofermentans PYCC 5603^T and Pichia guilliermondii PYCC 3012: influence of sugar and oxygen on product formation*. Applied Microbiology and Biotechnology, 2007. **75**:303-310.
36. Laplace, J. M., J. P. Delgenes, R. Moletta, and J. M. Navarro, *Alcoholic fermentation of glucose and xylose by Pichia stipitis, Candida shehatae, Saccharomyces cerevisiae and Zymomonas mobilis: oxygen requirement as a key factor*. Applied Microbiology and Biotechnology, 1991. **36**: 158-162.
37. Slininger, P. J., R. J. Bothast, M. R. Okos, and M. R. Ladisch, *Comparative evaluation of ethanol production by xylose-fermenting yeasts presented high xylose concentrations*. Biotechnology Letters, 1985. **7**: 431-436.
38. Ligthelm, M.E., B. A. Prior, and J. C. du Preez, *The oxygen requirements of yeasts for the fermentation of D-xylose and D-glucose to ethanol*. Applied Microbiology and Biotechnology, 1988. **28**: 63-68.

39. Yu, S., H. Jeppsson, and B. Hahn-Hägerdal, *Xylulose fermentation by Saccharomyces cerevisiae and xylose-fermenting yeast strains*. Applied Microbiology and Biotechnology, 1995. **44**: 314-320.
40. Barbosa, M. de F., H. Lee, *Plasma Membrane Mg²⁺-ATPase of Pachysolen tannophilus characterization and role in alcohol tolerance*. Applied and Environmental Microbiology, 1991. **57**: 1880-1885.
41. Lohmeier-Vogel, E. M., C. R. Sopher, H. Lee, *Intracellular acidifications as a mechanism for the inhibition by acid hydrolysis-derived inhibitors of xylose fermentation by yeasts*. Journal of Industrial Microbiology and Biotechnology, 1998. **20**: 75-81.
42. Watanabe, T., I. Watanabe, M. Yamamoto, A. Ando, T. Nakamura, *A UV-induced mutant of Pichia Stipitis with increased ethanol production from xylose and selection of a spontaneous mutant with increased ethanol tolerance*. Bioresource Technology, 2011. **102**: 1844-1848.
43. Ollson, L., B. Hahn- Hägerdal, *Fermentative performance of bacteria and yeast in lignocellulosic hydrolysates*. Proceedings in Biochemistry, 1993. **28**: 249-256.
44. Chiang, L.-C., C.-S. Gong, L.-F. Chen, and G. T. Tsau, *D-xylulose fermentation to ethanol by Saccharomyces cerevisiae*. Applied and Environmental Microbiology, 1981. **42**: 284-289.
45. Eliasson, A., E. Boles, B. Johansson, M. Osterberg, J. M. Thevelein, I. Spencer-Martin, H. Juhnke, and B. Hahn-Hägerdal, *Xylulose fermentation by mutant and wild-type strains of Zygosaccharomyces and Saccharomyces cerevisiae*. Applied Microbiology and Biotechnology, 2000. **53**: 376-382.
46. Kotter, P., and M. Ciriacy, *Xylose fermentation by Saccharomyces cerevisiae*. Applied Microbiology and Biotechnology, 1993. **38**: 776-783.
47. Bruinenberg, P. M., *The NADP(H) redox couple in yeast metabolism*. Antoine Van Leeuwenhoek, 1986. **52**: 411-429.

48. Walfriedsson M., J. Hallborn, M. Penttilä, S. KerDenen, and B. Hahn-Hägerdal, *Xylose-metabolizing Saccharomyces cerevisiae strains overexpressing the TKL1 and TAL1 genes encoding the pentose phosphate pathway enzymes transketolase and transaldolase*. Applied and Environmental Microbiology, 1995. **61**: 4184-4190.
49. Ho, N., and G. T. Tsao, *Recombinant yeasts for effective fermentation of glucose and xylose*. US patent 5789210.
50. Eliasson, A., C. Christensson, C. F. Wahlbom, and B. Hahn-Hägerdal, *Anaerobic xylose fermentation by recombinant Saccharomyces cerevisiae carrying XYL1, XYL2, and XKS1 in mineral medium chemostat cultures*. Applied and Environmental Microbiology, 2000. **66**: 3381-3386.
51. Wahlbom, C. F., W. H. van Zyl, L. J. Jonsson, B. Hahn-Hägerdal, and R. R. Otero, *Generation of the improved recombinant xylose-utilizing Saccharomyces cerevisiae TMB 3400 by random mutagenesis and physiological comparison with Pichia stipitis CBS 6054*. FEMS Yeast Research, 2003. **3**:319-326.
52. Matsushika, A., H. Inoue, K. Murakami, O. Takimura, and S. Sawayama, *Bioethanol production performance of five recombinant strains of laboratory and industrial xylose-fermenting Saccharomyces cerevisiae*. Bioresource Technology, 2009. **100**: 2392-2398.
53. Sonderegger, M., U. Sauer, *Evolutionary engineering of Saccharomyces cerevisiae for anaerobic growth on xylose*. Applied and Environmental Microbiology, 2003. **69**: 1990-1998.
54. Sonderegger, M., M. Jeppsson, C. Larsson, M.-F. Gorwa-Grauslund, E. Boles, L. Olsson, I. Spencer-Martin, B. Hahn-Hägerdal, and U. Sauer, *Fermentation performance of engineered and evolved xylose-fermenting Saccharomyces cerevisiae strains*. Biotechnology and Bioengineering, 2004. **87**: 90-98.
55. Zaldivar, J., A. Borges, B. Johansson, H. P. Smits, S. G. Villas-Boas, J. Nielsen, and L. Olsson, *Fermentation performance and intracellular metabolite patterns in laboratory and industrial xylose-fermenting Saccharomyces cerevisiae*. Applied Microbiology and Biotechnology, 2002. **59**: 436-442.

56. Petschacher, B., and B. Nidetzky, *Altering the coenzyme preference of xylose reductase to favour utilization of NADH enhances ethanol yield from xylose in a metabolically engineered strain of Saccharomyces cerevisiae*. Microbial cell factories, 2008. **7**:9.
57. Walfriedsson, M., X. Bao, M. Anderlund, G. Lilius, L. Bülow, and B. Hahn-Hägerdal, *Ethanol fermentation of xylose with Saccharomyces cerevisiae harbouring the Thermus thermophilus xylA gene, which expresses an active xylose (glucose) isomerase*. Applied and Environmental Microbiology, 1996. **62**: 4648-4651.
58. Kuyper, M., H. R. Harhangi, A. K. Stave, A. A. Winkler, M. S. Jetten, W. T. de Laat, J. J. den Ridder, H. J. Op den Camp, J. P. van Dijken, and J. T. Pronk, *High-level functional expression of a fungal xylose isomerase: the key to efficient ethanolic fermentation of xylose by Saccharomyces cerevisiae?* FEMS Yeast Research, 2003. **4**: 69-78.
59. Kuyper, M., A. A. Winkler, J. P. Dijken, and J. T. Pronk, *Minimal metabolic engineering of Saccharomyces cerevisiae for efficient anaerobic xylose fermentation: a proof of principle*. FEMS Yeast Research, 2004. **4**: 655-664.
60. Kuyper, M., M. M. Hartog, M. J. Toirkens, M. J. Almering, A. A. Winkler, J. P. Dijken, and J. T. Pronk, *Metabolic engineering of a xylose-isomerase-expressing Saccharomyces cerevisiae strain for rapid anaerobic xylose fermentation*. FEMS Yeast Research, 2005. **5**: 399-409.
61. Kuyper, M., M. J. Toirkens, J. A. Diderich, A. A. Winkler, J. P. van Dijken, and J. T. Pronk, *Evolutionary engineering of mixed-sugar utilization by a xylose-fermenting Saccharomyces cerevisiae strain*. FEMS Yeast Research, 2005. **5**:925-934.
62. Gueldener, U. S. Heck, T. Fiedler, J. D. Beinhauer, and J. H. Hegemann, *A new efficient gene disruption cassette for repeated use in budding yeast*. Nucleic Acids Research, 1996. **24**: 2519-2524.
63. Gueldener U., J. Heinisch, G. J. Koehler, D. Voss, and J. H. Hegemann, *A second set of loxP marker cassettes for Cre-mediated multiple gene knockouts in budding yeast*. Nucleic Acids Research, 2002. **30**: e23.

64. Gietz, R. D., R. H. Schiestl, A. R. Willems, and R. A. Woods, *Studies on the transformation of intact yeast cells by the LiAc/SS-DNA/PEG procedure*. *Yeast*, 1995. **11**: 355-360.
65. Costanzo, M. C., and T. D. Fox, *Transformation of yeast by agitation with glass beads*. *Genetics*, 1988. **120**: 667-670.
66. Boeke, J. D., F. LaCroute, and G. R. Fink, *A positive selection for mutants lacking orotidine- 5'-phosphate decarboxylase activity in yeast: 5-fluoro-orotic acid resistance*. *Molecular and general Genetics*, 1984. **197**: 345-346.
67. Jansen, G., C. Wu, B. Schade, D. Y. Thomas, M. Whiteway, *Drag&Drop cloning in yeast*. *Gene*, 2005. **344**: 43-51.
68. Shao, Z. H. Zhao, and H. Zhao, *DNA assembler, an in vivo genetic method for rapid construction of biochemical pathways*. *Nucleic Acids Research*, 2009. **37**, e16.
69. Sandmeyer S., *Integration by design*. *PNAS*, 2003. **100**: 5586-5588.
70. Boeke, J. D., and S. B. Sandmeyer, *Yeast transposable elements in the molecular and cellular biology of the yeast Saccharomyces: Genome dynamics, protein synthesis, and energetic*. 1991, pp. 193-261. Cold Spring Harbor Laboratory Press, Cold Spring Harbor, New York.
71. Davis, R. H., and F. J. de Serres, *Genetic and microbiological engineering techniques for Neurospora crassa*. *Methods in Enzymology*, 1970. **17**: 79-143.
72. Ostergaard, S., L. Olsson, and J. Nielsen, *Metabolic engineering of Saccharomyces cerevisiae*. *Microbiology and Molecular Biology Reviews*, 2000. **64**: 34-50.
73. Stafford, D. E., and G. Stephanopoulos, *Metabolic engineering as an integrating platform for strain development*. *Current Opinions in Microbiology*, 2001. **4**: 336-340.
74. Bailey, J. E., *Lessons from metabolic engineering for functional genomics and drug discovery*. *Nature Biotechnology*, 1999. **17**: 616-618.
75. Patnaik, R., S. Louis, V. Gavrilovic, K. Perry, W. P. C. Stemmer, C. M. Ryan, and S. del Cardayre, *Genome shuffling of Lactobacillus for improved acid tolerance*. *Nature Biotechnology*, 2002. **20**: 707-712.

76. Rohlin, L., M.-K. Oh, and J. C. Liao, *Microbial pathway engineering for industrial processes: evolution, combinatorial biosynthesis and rational design*. Current Opinion in Microbiology, 2001. **4**: 330-335.
77. Sauer, U., *Evolutionary engineering of industrially important microbial phenotypes*. Advances in Biochemical Engineering/ Biotechnology, 2001. **73**: 129-170.
78. Zelder, O., and B. Bauer, *Environmentally directed mutations and their impact on industrial biotransformation and fermentation processes*. Current Opinion in Microbiology, 2000. **3**: 248-251.
79. Ho, N. W. Y., Z. Chen, and A. P. Brainard, *Genetically engineered Saccharomyces yeast capable of effective cofermentation of glucose and xylose*. Advances in Environmental Microbiology, 1998. **64**: 1852-1859.
80. Hahn-Hägerdal, B., C. F. Wahlbom, M. Gardonyi, W. H. van Zyl, R. R. Cordero Otero, and L. J. Jönsson, *Metabolic engineering of Saccharomyces cerevisiae for xylose utilization*. Advances in Biochemical Engineering/ Biotechnology, 2001. **73**: 53-84.
81. Ho, N. W. Y., Z. Chen, A. P. Brainard, and M. Sedlak, *Successful design and development of genetically engineered Saccharomyces yeasts for effective cofermentation of glucose and xylose from cellulosic biomass to fuel ethanol*. Advances in Biochemical Engineering/ Biotechnology, 1999. **65**: 163-192.
82. Bengtsson, O., M. Jeppsson, M. Sonderegger, N. Skorupa Parachin, U. Sauer, B. Hahn- Hägerdal, M.-F. Gorwa-Grauslund, *Identification of common traits in improved xylose-growing Saccharomyces cerevisiae for inverse metabolic engineering*. Yeast, 2008. **25**: 835-847.
83. Wisselink, H. W., M. T. Toirkens, Q. Wu, J. T. Pronk, A. J. van Maris, *Novel evolutionary engineering approach for accelerates utilization of glucose, xylose, and arabinose mixtures by engineered Saccharomyces cerevisiae strains*. Applied and Environmental Microbiology, 2009. **75**: 907-914.

84. Karhumaa, K., B. Hahn- Hägerdal , M.-F. Gorwa-Grauslund, *Investigation of limiting metabolic steps in the utilization of xylose by recombinant Saccharomyces cerevisiae using metabolic engineering*. Yeast, 2005. **22**: 359-368.
85. Karhumaa, K., R. Garcia Sanchez, B. Hahn- Hägerdal , M.-F. Gorwa-Grauslund, *Comparison of the xylose reductase-xylitol dehydrogenase and the xylose isomerase pathways for xylose fermentation by recombinant Saccharomyces cerevisiae*. Microbial Cell Factories, 2007. **6**: 5
86. Tanino, T., A. Hotta, T. Ito, J. Ishii, R. Yamada, T. Hasunuma, C. Ogino, N. Ohmura, T. Ohshima, A. Kondo, *Construction of a xylose-metabolizing yeast by genome integration of xylose isomerase gene and investigation of the effect of xylitol on fermentation*. Applied Microbiology and Biotechnology, 2010. **88**: 1215-1221.
87. Krahulec, S., B. Petschacher, M. Wallner, K. Longus, M. Klimacek, B. Nidetzky, *Fermentation of mixed glucose-xylose substrates by engineered strains of Saccharomyces cerevisiae: role of the coenzyme specificity of xylose reductase, and effect of glucose on xylose utilization*. Microbial Cell Factories, 2010. **9**:16.

